Solid State Phenomena Vol. 189 (2012) pp 209-232
Online available since 2012/Jun/04 at www.scientific.net

doi:10.4028/www.scientific.net/SSP.189.209

Y-type Hexaferrites: Structural, Dielectric and Magnetic Properties

Rajshree B. Jotania[1,a] and Hardev S. Virk [2,b]

[1]Department of Physics, University School of Science, Gujarat University,

Navrangpura, Ahmedabad 380 009, India

[2]Eternal University, Baru Sahib, Himachal Pradesh, India

[a]rbjotania@gmail.com, [b]hardevsingh.virk@gmail.com

Keywords: Hexaferrites, Y-type hexaferrites, synthesis, characterization, dielectric properties, magnetic properties

Abstract. This paper attempts to provide a historical survey of structure of various types of hexaferrites. It provides information about synthesis, characterization, structural, magnetic and dielectric properties of Y-type hexagonal ferrites using various chemical routes. We have prepared a series of cobalt doped $Sr_2Cu_{2-x}Co_xFe_{12}O_{22}$ (x = 0.0 to 1.0) hexaferrites using a wet chemical co-precipitation technique. The prepared hexaferrite precursors were calcined at 950 ºC for 4 hours in a furnace and slowly cooled to room temperature. The crystal structure of Y-type hexaferrites is rather complicated. The chemical and structural changes were examined in detail by X-ray diffraction (XRD), Differential scanning calorimetry (DSC), Scanning electron microscopy (SEM), and Fourier transform infra-red (FTIR) spectroscopy. X-ray diffraction studies showed that sintering temperature as low as 950°C was sufficient to produce a single-phase Y-type hexaferrite material. The dielectric measurements were carried out over the frequency range of 100 Hz to 2 MHz at room temperature using an LCR meter to study the variation of dielectric constant and loss tangent with frequency. The magnetic properties of hexaferrite samples were investigated using a vibration sample magnetometer (VSM), and a superconducting quantum interference device (SQUID) magnetometer in the temperature range 30K to 200K. A change from ferromagnetic state to super paramagnetic state has been observed in Co doped $Sr_2Cu_{2-x}Co_xFe_{12}O_{22}$ (x= 0.6 to 1.0) hexaferrite. The novel applications of all types of hexaferrite materials have been described.

1. Introduction

Richard Feynman [1] once stated that ferrites were one of the most difficult areas for theoretical description but the most interesting for studies and practical applications. These words are especially true when dealing with hexaferrites or hexagonal ferrites, which have a hexagonal crystallographic structure. The world's first permanent magnets were based on hexagonal barium ferrite $BaFe_{12}O_{19}$ (ferroxdure, BaM) - appeared in 1951 [2], which paved the way for a large spin–orbit coupling. The main engineering problem that was solved at that time was the replacement of metallic Ni- and Co- alloy magnets by comparatively compact and lightweight permanent magnetic systems. The systematic study and applications of gyromagnetic properties of hexaferrites started in 1955 [3-5]. Since the last 60 years enormous progress in fundamental, theoretical and experimental laboratory studies of various properties of hexaferrites, their synthesis, and engineering of a wide range of microwave and mm-wave coatings and devices on their basis, has been achieved.

Hexagonal ferrites are very attractive materials for high frequency circuits and operating devices. They are widely used as permanent magnets, high-density perpendicular and magneto-optical recording media and micro-wave devices. Barium hexagonal ferrites are suitable candidates for high density, over coat free, contact or semi contact recording media [6]. On account of their superior chemical stability, mechanical hardness, excellent corrosion and wear resistance, low level of media noise and high Curie temperature, they are suitable for rigid disk media without protective and lubricant layers. Due to large magneto-crystalline anisotropy and strong dependence of the orientation of easy axis on the microstructure, they have potential for application in both perpendicular and longitudinal magnetic recording media [7-9].

2.0 Classification of Hexaferrites

Magnetic oxide, known as a "magnetoplumbite", has a hexagonal structure from the mineral. It has a major preferred axis called the c-axis and a minor axis called the a-axis. The oxygen ions are closely packed as they are in the spinel structure but there are oxygen layers which include the Ba^{2+}, Sr^{2+} or Pb^{2+} ions of the same ionic radii as the oxygen ions and therefore can replace them in the lattice. There are other ferromagnetic oxides also available all of which can be derived by combining the ferrite spinel ($MeO{\cdot}Fe_2O_3$) and ferroxdure ($BaO{\cdot}6Fe_2O_3$) using the chemical composition diagram shown in Fig. 1. The same is true with chemical formula for each type, namely, M, Y, W, Z, X, and U, as given in Table 1 [10-13].

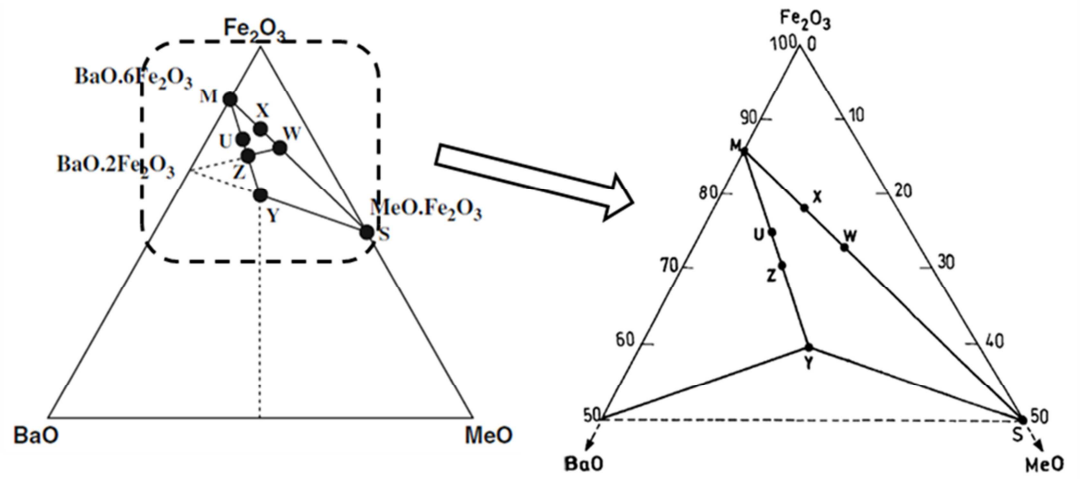

Fig.1 Chemical compositional BaO-MeO-Fe_2O_3 ternary phase diagram showing how the different hexagonal ferrites are derived [14].

Table 1 Hexaferrite types with their chemical formula, composition and stacking order

Hexaferrites Type	Chemical Formula	Composition	Stacking order[#]
S-Spinel	$2\ Me^{2+}{\cdot}2Fe_2O_4$	$2MeO{\cdot}2Fe_2O_3$	
M	$Ba^{2+}Fe_{12}O_{19}$	$BaO{\cdot}6Fe_2O_3$	RSR*S*
Y	$Ba^{2+}{}_2Me^{2+}{}_2Fe_{12}O_{22}$	$2BaO{\cdot}2MeO{\cdot}6Fe_2O_3$	TSTST
W	$Ba^{2+}Me^{2+}{}_2Fe_{16}O_{27}$	$BaO{\cdot}2MeO{\cdot}8Fe_2O_3$	RSSR*S*S*
Z	$Ba^{2+}{}_3Me^{2+}{}_2Fe_{24}O_{41}$	$3BaO{\cdot}2MeO{\cdot}12Fe_2O_3$	RSTSR*S*T*S*
X	$Ba^{2+}{}_2Me^{2+}{}_2Fe_{28}O_{46}$	$2BaO{\cdot}2MeO{\cdot}14Fe_2O_3$	RSR*S*S*
U	$Ba^{2+}{}_4Me^{2+}{}_2Fe_{36}O_{60}$	$4BaO{\cdot}2MeO{\cdot}18Fe_2O_3$	RSR*S*T*S*

[#]Sub-units for stacking order, using, S = Fe_6O_8 (spinel), R = $BaFe_6O_{11}$ (hexagonal), and T = $Ba_2Fe_8O_{14}$ (hexagonal). The asterix (*) indicates that the corresponding sub-unit is rotated 180° around the hexagonal axis.

Thus hexagonal ferrites are divided into six different types according to chemical composition and crystal structure: $M(AFe_{12}O_{19})$, $W(AMe_2Fe_{16}O_{27})$, $X(A_2Me_2Fe_{28}O_{46})$, $Y(A_2Me_2Fe_{12}O_{22})$, $Z(A_3Me_2Fe_{24}O_{41})$, $U(A_4Me_2Fe_{36}O_{60})$; where A = Ba^{2+}, Sr^{2+}, La^{2+}, Pb^{2+} and Me = a bivalent transition metal [13].

2.1 M-type Hexaferrites. Magnetoplumbite – structured ferrites having a generic formula $MeO{\cdot}6Fe_2O_3$, where Me represents a divalent ion such as Ba^{2+}, Sr^{2+}, or it has hexagonal structure composed of stacked spinel ionic layers with interspaced ionic layers of M^{2+}, O^{2-} and Fe. These types of oxide ferrites have extensive magnetocrystalline anisotropy due to their low crystal symmetry.

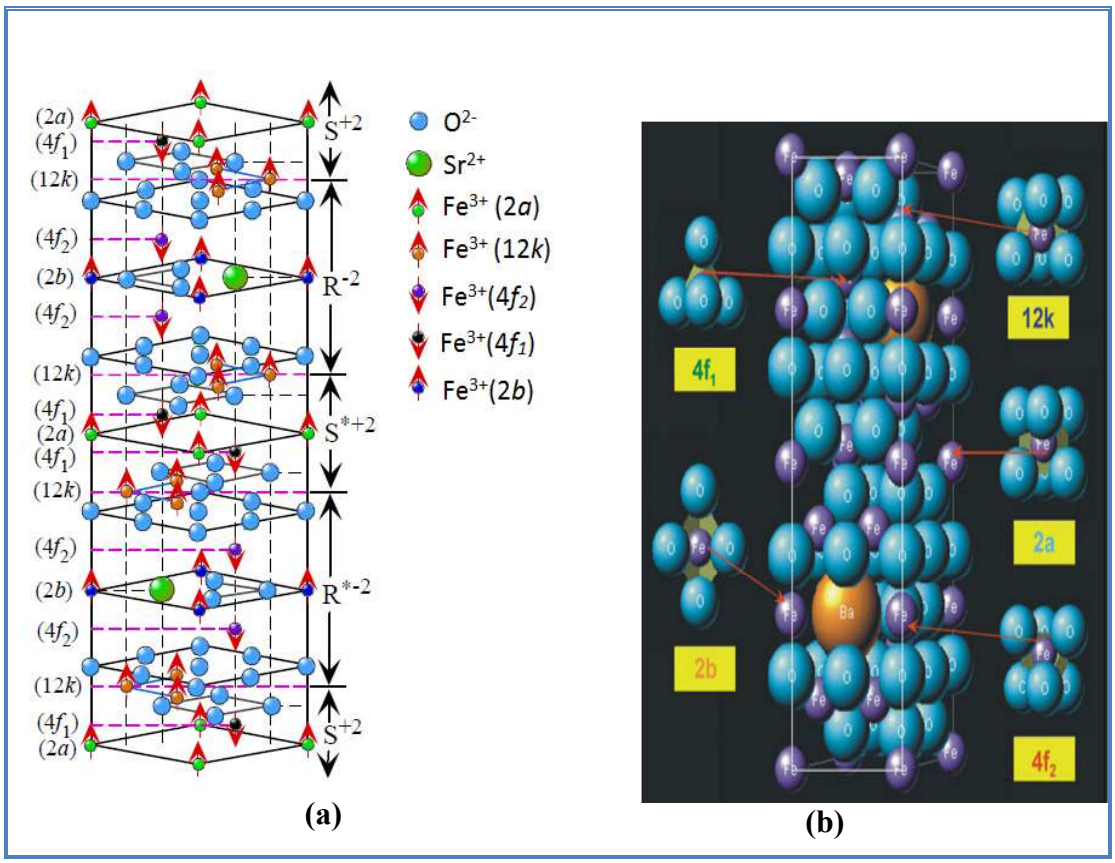

Fig. 2 (a) Crystal structure of hexagonal *M*-type hexaferrite, and (b) along with the five Fe sites with their surroundings [13, 15].

Figure 2 (a) shows the schematic structure of the hexaferrite, $SrFe_{12}O_{19}$. The M-type ferrite crystallizes in a hexagonal structure with 64 ions per unit cell on 11 different symmetry sites ($P6_3/mmc$ space group). The 24 Fe^{3+} atoms are distributed over five distinct sites: three octahedral sites (12*k*, 2*a* and 4f_2), one tetrahedral (4f_1) site and one hexahedral (trigonal bipyramidal) site (2*b*) (Table 2, Fig 2 (b)).The arrows on Fe ions represent the direction of spin polarization. The unit cell contains a total of 38 O^{2-} ions, 2 Sr^{2+} ions, and 24 Fe^{3+} ions. Fe^{3+} ions in 12*k*, 2*a*, and 2*b* sites (16 total per unit cell) have their spins up, while the Fe^{3+} ions in 4f_1 and 4f_2 sites (8 total per unit cell) have their spins down, which results in a net total of 8 spins up, and therefore, a total moment of (8 x 5)μ_B = 40μ_B per unit cell that contains two Sr^{2+} ions. The asterix (*) indicates that the corresponding sub-unit is rotated 180° around the hexagonal axis. Strontium hexaferrite, $SrFe_{12}O_{19}$, is a ferri-magnetic material in which iron ions are coupled anti ferro-magnetically among five different crystallographic sites. This ferri-magnetic material exhibits a high saturation magnetization and high coercivity because of the relatively high magneto-crystalline anisotropy field.

The structure of M-type hexagonal is stacked alternatively by spinel (S = $Fe_6O_8^{2+}$) and hexagonal (R = $MFe_6O_{11}^{2-}$) layers. The O^{2-} ions exist as close-packed layers, with the M^{2+} substituting for an O^{2-} in the hexagonal layer. The three parallel (2*a*, 12*k* and 2*b*) and two antiparallel (4f_1 and 4f_2) sub-lattices, which are coupled by super-exchange interactions through the O^{2-} ions, form the ferrimagnetic structure [16, 17]. A schematic M-type structural representation and the surroundings of five Fe^{3+} sites are shown in Fig. 2 (b) [18]. M-type hexaferrites have two types of anisotropy, c-axis anisotropy and c-plane anisotropy, which are associated with the easy magnetization along the c-axis and in the c -plane, respectively.

Table 2 Number of Fe^{3+} ions in sublattices of hexaferrites and their spin [11]

Sr. No	Site	Geometry	No. of Fe^{3+} ions	Spin
1	12k	Octahedral	6	Up
2	2a	Octahedral	1	Up
3	$4f_1$	Tetrahedral	2	Down
4	$4f_2$	Octahedral	2	Down
5	2b	Trigonal bipyramidal	1	Up

The magnetoplumbite unit cell (Fig. 3) contains a total of ten layers (the length of c-axis is 23.2 Å and of a-axis is 5.88 Å), two of which contain the Ba^{2+} (or Sr^{2+}) ions: four layers of four oxygen ions each; followed by a layer of three oxygen ions and one Ba^{2+} ion; again followed by the same sequence but situated diametrically opposite to the Ba^{2+} ion in the previous layer containing Ba^{2+}. The Fe^{3+} ions are located in the interstices of these ten layers. There are octahedral and tetrahedral sites plus one more type not found in the spinel structure in which the metal ion is surrounded by 5 oxygen ions forming a trigonal bi- pyramid in the same layer as the Ba^{2+} ion. The arrows indicate the spin orientations and the drawn vertical lines are axis of three fold symmetry. A cross indicates the center of symmetry and all layers containing barium are mirror planes and are denoted by 'm' in the figure 3. In an elementary cell each layer contains four large ions. There are always four oxygen ions in four successive layers but each fifth layer contains three oxygen ions and one barium ion. Table 3 represents the classification of ionic sites by blocks and by relative orientation of magnetic moments in Barium hexaferrites.

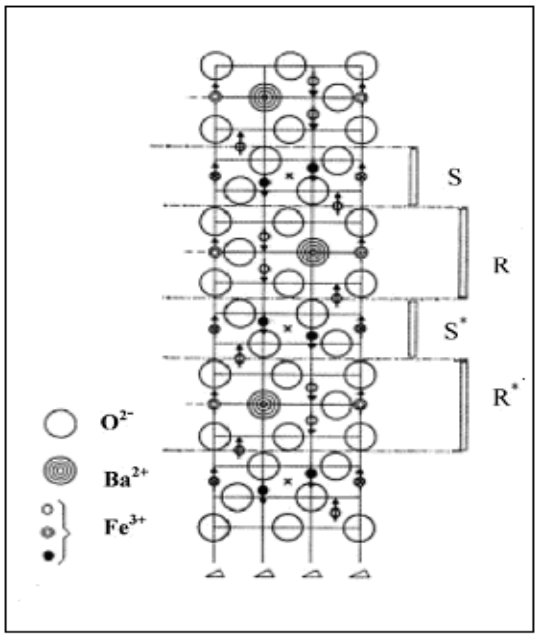

Fig. 3 Unit cell of the M-type hexaferrite [17].

Table 3 Classification of ionic sites by blocks and by relative orientation of magnetic moments in Barium hexaferrites

Sites	Blocks	Site types	Relative direction of Magnetic moments
Fe 1	S	Octahedral	Up
Fe 2	R	Bipyramidal	Up
Fe 3	S*	Tetrahedral	Down
Fe 4	R*	Octahedral	Down
Fe 5	R/S	Octahedral	Up

Barium and Strontium hexaferrites possess structure of M-type. Strontium ferrite is almost identical to $BaFe_{12}O_{19}$ in its crystallographic structure and magnetic properties, except that the sintered magnets generally have higher coercivity. The magnetic moments of the iron ions (Fe^{3+}) which lie along the c-axis are coupled to each other by a super-exchange interaction. The angle between the ferric cations and oxygen in Fe-O-Fe bonds determines their antiferromagnetism (i.e., larger exchange for larger angles). The ferromagnetic resonance (FMR) line width for a single crystal is reported to range from 10 to 20 Oe [18, 19]. The FMR linewidths of M-type hexaferrites are much larger than those of Yttrium Iron Garnet (YIG), i.e. up to ΔH = 50 Gauss for the best material against ΔH = 0.5 Gauss for Yttrium Iron Garnet. With proper design and substitutions, passive elements including mm-wave circulators can be constructed from hexaferrites. The M-type Sr-hexaferrites are used in magneto-optical devices. The measurement of DC electrical resistivity is very useful to judge the applications of Sr-hexaferrite in the microwave devices. If the material shows high values of DC resistivity then it is beneficial for its use in microwave device. The best-known member is the uniaxial permanent magnet of M-type $BaFe_{12}O_{19}$ (Ferroxdure), and the analogous $SrFe_{12}O_{19}$. The Ba-ferrite has an anisotropy field of 17 kG. The presence of large Ba ions and the slightly modified crystal structure causes the hexaferrites to have hard magnetic properties, unlike spinels and garnets [20]. The researchers are also interested to fabricate the Sr-hexaferrite with high resistivity.

M-type hexaferrites are widely used materials in fabrication of permanent magnets, which account for about 90 wt% of the annual production of permanent magnets because of their low price combined with reasonable magnetic performances. They have found numerous technical applications in microwave devices at mm wave frequencies. Radar absorbing paint made from ferrites is used to coat military aircraft for spying operation. The permanent magnetic materials are also used in loudspeakers, plasto-ferrites, injection-molded pieces, microphones, permanent magnetic motors and moving-coil instruments such as galvanometers, ammeters and voltmeters. Magnetic motors have many applications, like windshield-wipers, heater fans etc. in automobiles, and like electric carving knives, electric tooth brushes etc. in home appliances. Microwaves in the higher gigahertz range are being increasingly utilized in wireless communication, radar, local area network, secret system, satellites communication, precise guidance system and remote sensing techniques. Electromagnetic interface (EMI) is also becoming a serious problem and a matter of crucial concern in higher gigahertz range along with the development of higher gigahertz electronics and the trend towards miniature circuitry. The reduction of electromagnetic backscattering using the microwave absorbing materials therefore has important implications in the field of electromagnetic compatibility. Microwave absorbers are also in high demand for defense use. Application of microwave absorbing coating on the exterior surface of military aircraft and vehicles helps avoid detection by radar. The M-type hexaferrites due to their large tunable anisotropy field are extensively exploited in the recent years in higher gigahertz range [21-26].

2.2 W-type Hexaferrites. The Me_2W (W-type) $BaMe_2Fe_{16}O_{27}$ hexaferrite was discovered in the Philips' research laboratories in 1980 [27]. It exhibits a magnetic uniaxial anisotropy along the c-axis of the hexagonal structure as in the case of the M-type hexaferrite. More and more attention has been devoted to these hexaferrites in the past decades because of their moderate magnetic properties, excellent chemical stability, low cost, high coercivity and large magnetic energy product [28-34].

The W-type structure consists of one Ba- containing layer for every seventh oxygen layer of the spinel structure and is thus closely related to the M structure. Substitution of different combinations of divalent metal ions paves the way for changing the saturation magnetization and Néel temperature of the W hexaferrite. The crystal structure of W-type hexagonal ferrite is very complex and can be considered as superposition of R and S blocks (where R = $BaFe_6O_{11}^{2-}$ is hexagonal and S =$Fe_6O_8^{2+}$ is cubic spinel) along the hexagonal c-axis with a structure of RSSR*S*S*, where R is three oxygen layer block with composition $BaFe_6O_{11}$, S (Spinel block) is a two oxygen layer block with composition Fe_6O_8 and '*' means the respective block is turned 180° around the hexagonal axis. The O^{2-} ions exist as close packed layers, one Ba^{2+} ion is found replacing an O^{2-}ion in R block, the Fe^{3+} ions are distributed in five different interstitial sublattices (Figs. 4 & 5).

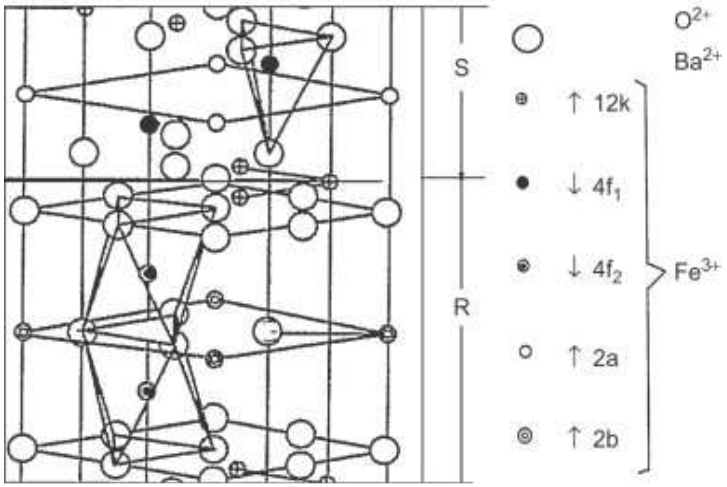

Fig. 4 Diagram representation of the S and R blocks [18].

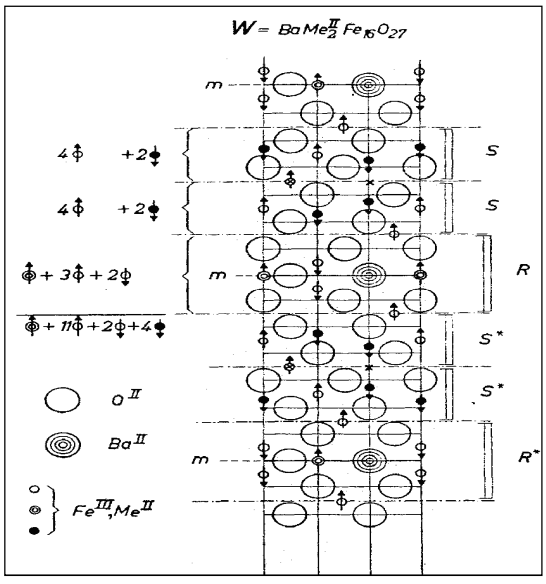

Fig. 5 The elementary unit cell of W- type hexaferrites [18].

W-type hexaferrite is a very useful material for home appliances, electronic products, communication equipments, permanent magnets, recording heads, bubble domain memories, components in high-frequency microwave devices and data processing devices due to its unique electrical and magnetic properties [35–39]. The structural and magnetic properties of W-type hexaferrite depend on many factors like method of preparation, sintering temperature, type and amount of substitution etc. [40-44]. W-type ferrites $AMe_2Fe_{16}O_{27}$ (*Me* = Mg, Mn, Fe, Co, Ni, Cu, Zn) can undergo spin reorientation transitions (SRT) between different anisotropy configurations (easy plane ↔ easy cone ↔ easy axis) induced by change of temperature or applied magnetic field [45–52]. The transition temperatures can be tuned by modifying the chemical composition (substitution of bivalent metal *M*). Moreover, some SRT are expected to be of the first order, which suggests a potential application of W-type ferrites in room temperature magnetic refrigeration [53].

The cations in W-type hexaferrites occupy seven non-equivalent sub-lattices, i.e. 12k, $4f_{VI}$, 6g, 4f (octahedral coordination), 4e, $4f_{IV}$ (tetrahedral coordination) and 2d (bipyramidal coordination) [54-56]. All these sub-lattices are present in different number of R-blocks (Ba containing layer) and S-blocks (spinel layer) that construct W-type ferrites [18]. However, there are only five magnetically non-equivalent sub-lattices from magnetic perspective, i.e. 4e and $4f_{IV}$ that merge into f_{IV} magnetic sub-lattice while 6g and 4f combine to 2b sub-lattice and called as b magnetic sub-lattice (Table 4) [57].

Table 4 Coordination, spin direction, block location and number of iron ions for each site of W-type hexaferrites

Magnetic site	Crystallographic site	Co-ordination	Spin	Block	Number
f_{VI}	4 f_{VI}	octahedral	down	R	2
a	6g 4f	octahedral	Up Up	S-S S	3 2
f_{IV}	4e $4f_{IV}$	tetrahedral	down down	S S	2 2
k	12k	tetrahedral	Up	R-S	6
b	2d	hexagonal	Up	R	1

The physical and magnetic properties of ferrites depend upon various factors like method of preparation, chemical composition, sintering temperature and time, type and amount of substitutions, etc. [58].

2.3 X-type hexaferrites. X-type hexaferrite possesses a chemical formula of $Ba_2Me_2Fe_{28}O_{46}$ and has been discovered over 50 years ago. The crystal structure of $Ba_2Fe_{30}O_{46}$ with real space coordinates for oxygen, barium, and transition metal ions was reported by Braun [59]. X-type is one kind of hexagonal ferrites whose structure can be considered as a stacking of R- and S-blocks along the hexagonal c-axis with a model as RSRSSR*S*R*S*S*, where R is a three-oxygen layer block with composition $BaFe_6O_{11}$, S (spinel block) a two-oxygen-layer block with composition Fe_6O_8, and the asterisk means that the corresponding block has been turned 180° around the hexagonal axis. X-type phases are usually seen mixed with M-type and W-type phases, and are difficult to separate. The X-type hexaferrite, X = 2M+S, is formed by stacking of R- and S-blocks (as shown in Table 5) along the hexagonal *c* axis. Three octahedral cation sites are located at the border between the R- and S-blocks and between the S-S blocks. There are two octahedral sites and a trigonal bipyramidal site in an R-block, whereas there are two tetrahedral sites and an octahedral site in an S-block. The elementary cell (a = 5.88 Å, c = 84.11 Å, density ρ = 5.30 g/cm^3) contains three chemical formula units (Z = 3). The unit cell consists of four alternative layers of the M and W structures belonging to the space symmetry $R\bar{3}m$ [60, 61].

Table 5 Crystallographic and magnetic characteristics of the metallic sublattices in the X-type $BaMe_2Fe_{28}O_{46}$ hexagonal ferrites

Block	Coordination	Number per block	Expected spin direction
R	Octahedral	2	Down
R	Trigonal bipyramidal	1	Up
R-S	Octahedral	3	Up
S	Octahedral	1	Up
S	Tetrahedral	2	Down
S-S	Octahedral	3	UP

2.4 Y-type hexaferrites. The crystal structure of Y-type $Ba_2Me_2Fe_{12}O_{22}$ is shown schematically in Fig. 6, with c- axis vertical [62]. These ferrites have a crystalline structure consisting of blocks having a spinel structure, with blocks containing *Ba*-O laminated alternately on top of each other. The space group is a rhombohedral crystal $R\bar{3}m$, and therefore each spinel layer and *Ba*-O block is repeated three times in a practical unit cell of the hexagonal setting. Since *Ba* represents alkaline-earth metal and *Me* represents divalent ions like Mg or Zn, the average valence of the Fe ion is three with oxygen positioned at the vertices of an octahedron or a tetrahedron. Although anti-ferromagnetic exchange interactions occur between adjacent Fe^{3+} ions, a complex magnetic structure can be observed as a result of some of the exchange interactions competing with each other. The anion frame work configuration in the Y-hexagonal ferrite consists of c- axis interleaving of two basis layers, the first containing only oxygen, the second having an ordered substitution of Ba for every fourth oxygen. The remaining smaller cations (Me^{2+} or Fe^{3+}) are at sites within anion frame work and can be neglected in treating the stacking relationship. The O and Ba-O layer interleave to form structural blocks; O, Ba-O, Ba-O, O. These two and four layers blocks are termed as S and T respectively. Further stacking gives the ST unit. The unit cell (Fig. 7) with hexagonal symmetry consists of 18 oxygen layers with a repeat distance extending through only six oxygen layers, the length of the c- axis being 43.56 Å. In the hexagonal element cell each layer again contains four large ions. There are four successive layers of four oxygen ions, followed by two layers each containing three oxygen ions and one barium ion. The unit cell is composed of the sequence STSTST including three formula units. The metallic cations are distributed among six sublattices as shown in Table 6. Three octahedral ions of sublattices $6c_{VI}$ and $3b_{VI}$ lie on a vertical threefold axis while the central $3b_{VI}$ ion sharing two faces of its coordination with the adjacent $6c_{VI}$ ions inside T block. Such a configuration possesses a higher potential energy of the structure due to a stronger electrostatic repulsion between the cations; therefore such sites are likely to be preferred by low charge ions.

Y-type hexagonal hexaferrites have gained much interest in recent years due to their multiferroic properties [63-65]. These ferrites are used in electronic communication, microwave devices and components [17, 66, 67]. Miniaturization of ferrite devices in the electronic communication requires high-permeability materials at relatively lower microwave frequencies (0–10 GHz) and Y-type hexaferrites are considered as potential materials for applications [68-73]. High permeability in Y-type ferrite is attributed to spin rotation and domain wall motions. Y-type hexaferrite is an important type of soft magnetic material in VHF and UHF [74].

Table 6 Number of ions per unit formula, coordination and spin orientation for the various metallic sublattices of Y-type structure [75]

Sublattice	Coordination	Block	Number of ions	Spin
$6c_{IV}$	tetrahedral	S	2	down
$3a_{VI}$	octahedral	S	1	UP
$8h_{VI}$	octahedral	S-T	6	UP
$6c_{VI}$	octahedral	T	2	down
$6c_{IV}$	tetrahedral	T	2	down
$3b_{VI}$	octahedral	T	1	UP

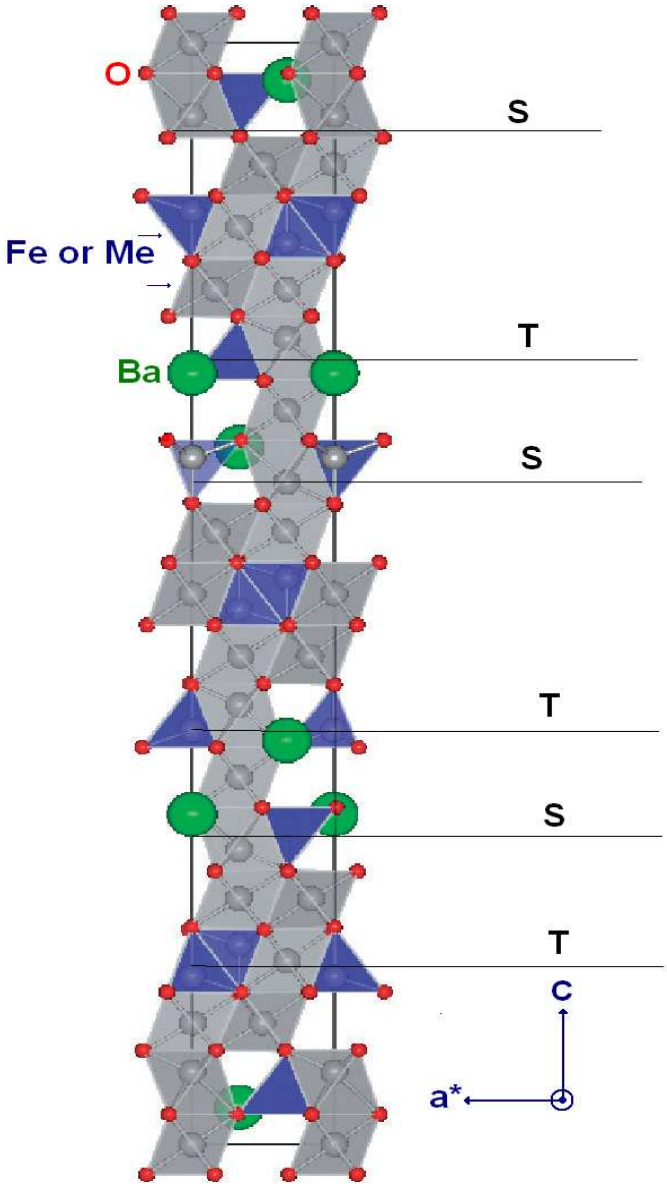

Fig. 6 Crystal structure of $Ba_2Me_2Fe_{12}O_{22}$ projected along the b axis. Large green and small red spheres represent Ba^{2+} and O^{2-} respectively. Fe^{3+} and Me^{2+} are randomly distributed in octahedral and tetrahedral sites. S and T are magnetic blocks, in which magnetic moments of Fe^{3+} are collinearly aligned [62].

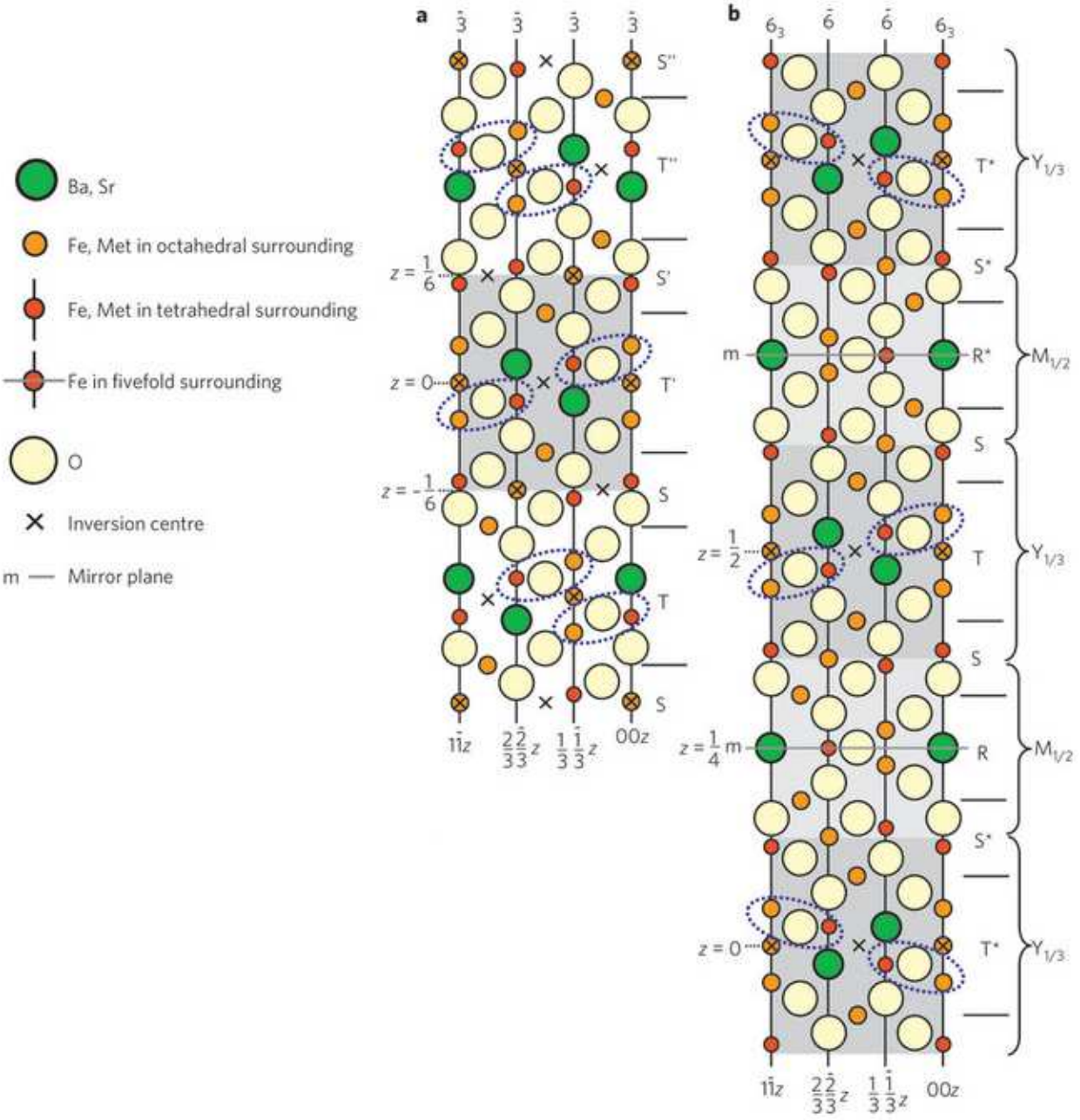

Fig. 7 Unit cell cross-sections of (a) Y-type, and (b) Z-type hexaferrites [76].

2.5 Z-type hexaferrites. Z-type hexaferrite is one of the most complex compounds in the family of hexaferrites and it has high permeability up to the GHz region, great resistivity, and good chemical and thermal stability. Z-hexaferrite is regarded as a sum of M- ($BaFe_{12}O_{19}$) and Y- ($Ba_2Me_2Fe_{12}O_{22}$) type hexaferrites. The crystal structure contains 33 close-packed layers, stacked along the hexagonal *c*-axis, and ordered in units called S, R, T blocks [77]. The unit cell cross section of Z-type hexaferrite is shown in Fig. 7.The unit cell of a Z-type hexaferritre contains 140 atoms and belongs to the $P6_3/mmc$ space group. Metal ions like Fe^{3+}, Co^{2+}, Zn^{2+} and Cu^{2+} are located in non-equivalent interstitial sites.

Z-type hexaferrite has great potential applications as anti-EMI material , radar absorbing materials (RAM) for magnetic devices in the GHz region. These ferrites are very useful for inductor cores or in UHF communications in the microwave region because of a ferromagnetic resonance at GHz frequencies [78, 79].

2.6 U-type hexaferrites. U-type hexaferrite, $Ba_4Me_2Fe_{36}O_{60}$ (Me_2U, Me = Cu, Fe, Co, Mn, Mg etc.) has the most complex crystal structure and the largest unit cell size. U-type hexaferrites are difficult to prepare in the single-phase condition due to their complex crystal structure. Compositionally and structurally, they are a superposition of M and Y-blocks along c-axis and their crystal structure is described by the stacking sequence RSR*S*TS* with the space group $R\bar{3}m$. The unit cell of the U-type compound formed by three molecules possesses the rhombohedral structure belonging to space group $R\bar{3}m$. The structure is built up by the superposition of two M-blocks and one Y-block along the c-axis. U-type hexaferrites possess excellent electromagnetic properties within the microwave region of the electromagnetic spectrum. U-hexaferrites are an interesting material for millimeter wave applications [20, 80-87].

3.0 Experimental Investigations of Y-type Hexaferrites

The structural properties of Y-type hexaferrite depend on many factors like preparation methods, sintering temperature, time, chemical composition and amount of substitution etc. Many studies have been reported on addition of divalent, trivalent and tetravalent ions in Y-hexaferrites [88-90]. Coexistence of the ferroelectric polarization and spontaneous magnetization has been studied in multiferroic Y-type hexaferrite, $Ba_2Mg_2Fe_{12}O_{22}$, by K. Taniguchi et al. [62]; where as two distinct ferroelectric phases in this multiferroic Y-type hexaferrite have been studied by Sagayama et al. [91]. Y-type Ba-hexaferrite ($Ba_2Zn_2Fe_{12}O_{22}$) powder has been studied well [92, 93] because it has potential to serve as an electromagnetic wave absorber in the GHz band. Y-type barium ferrite has c-plane anisotropy, while the others have c-axis anisotropy, but substitution of some elements can modify the anisotropy from c axis to c-plane. A soft mechano-chemical method has been used to prepare Y-type $Ba_2Co_2Fe_{12}O_{22}$ hexaferrites precursors [94]. The effects of particle size and concentration on microwave absorbing properties of Y-type hexaferrites, $Ba_2Cu_xCo_{2-x}Fe_{12}O_{22}$ (x =0.1), have been investigated in detail by Li et al. [95]. We have prepared a series of cobalt doped $Sr_2Cu_{2-x}Co_xFe_{12}O_{22}$ (x = 0.0 to 1.0) hexaferrite samples by using a wet chemical co-precipitation technique. The prepared hexaferrite precursors were calcined at 950 ºC for 4 hours in a furnace and slowly cooled to room temperature. The synthesis, characterization, structural, dielectric and magnetic properties of prepared Y-type hexagonal ferrites have been investigated and reported in the following sections.

3.1 Synthesis of $Sr_2Cu_{2-x}Co_xFe_{12}O_{22}$(x=0.0 to 1.0) Hexaferrites. Single-phase powders of $Sr_2Cu_{2-x}Co_xFe_{12}O_{22}$ hexaferrite were produced by utilizing a co-precipitation technique. A. R. Grade powders of strontium nitrate ($Sr(No_3)_2.6H_2O$), ferric nitrate ($Fe(NO_3)_2.9H_2O$), copper nitrate Cu $(NO_3)_2$ and cobalt nitrate **(**$Co(NO_3)_2{\cdot}4H_2O$) were used as starting materials and mixed in an appropriate amount of de-ionized water. Prepared mixture was stirred at 150 rpm for 2 h. Ammonium solution (w/v=30%) was added slowly in the mixture to adjust pH of 11. The mixed solution was stirred for two hours and was kept at room temperature 24 hours for aging. In order to lower the sintering temperature of the material, smaller particles were desired. The obtained precipitates were washed in 1:1 mixture of methanol and acetone followed by 100% de- ionized water to remove impurities. After precipitation, which occurred over a period of 2 h, the resultant powders were filtered utilizing vacuum filtration to remove water. The precipitate was dried at 80°C for 24 h in an oven and then calcined at 950°C for 4 hours, followed by furnace cooling to room temperature to get final product of $Sr_2Cu_{2-X}Co_XFe_{12}O_{22}$ hexaferrite particles. Figure 8 shows the schematic representation for the preparation of $Sr_2Cu_{2-X}Co_XFe_{12}O_{22}$ hexaferrite particles.

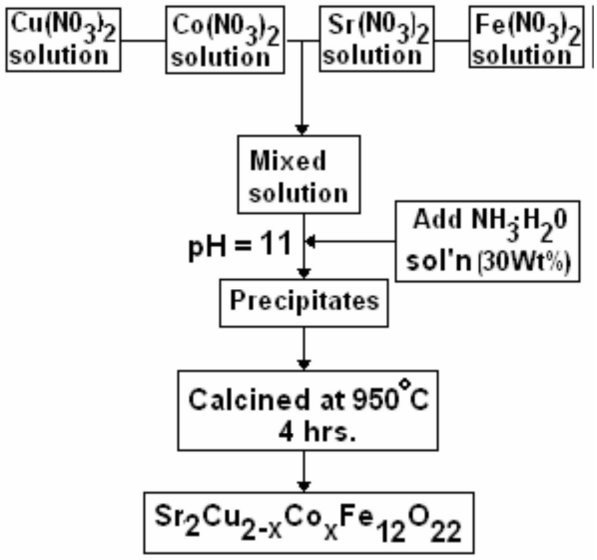

Fig. 8 Schematic representation for the preparation of $Sr_2Cu_{2-X}Co_XFe_{12}O_{22}$ hexaferrite particles.

3.2 Structural Characterization. The structural characterization of $Sr_2Cu_{2-x}Co_xFe_{12}O_{22}$ (x = 0.0 to 1.0) hexaferrite samples was carried out by the X-ray diffraction (XRD), Differential scanning calorimetry (DSC), Fourier Transform Infrared Spectroscopy (FT-IR) and Scanning Electron Microscopy (SEM) techniques. Dielectric properties, like dielectric constant and loss tangent, of prepared samples were measured between frequency ranges of 100 Hz to 2 MHz at room temperature. Phase identification and crystallite size of the calcined powder were determined using XRD analysis. The stretching of the M-O band was confirmed by FTIR analysis. The morphology of prepared samples was examined by SEM.

3.2.1 XRD analysis. The phase purity of all samples was investigated on PW1830 diffractometer by means of X-ray diffraction (XRD), using Cu Kα radiation (λ= 1.5406Å) at 45 kV in the range of $2\theta = 20–90^{\circ}$. The X-ray diffraction pattern of $Sr_2Cu_{2-x}Co_xFe_{12}O_{22}$ (x = 0.0 to 1.0) synthesized using co-precipitation technique was obtained at room temperature. Figure 9 shows X-ray diffraction pattern and confirms single Y-type phase structure. Well defined sharp Bragg peaks indicate good crystalline quality of prepared samples. All XRD reflection peaks are indexed by applying a hexagonal crystal system and space group $P6_3/mmc$ (here planes [0012], [113], [110], [1013], [116], [119], [024], [0210] [300], [2113], [1025], [220], [3015] used for prepared samples). Powder-X software has been used and after indexing on standard XRD data, experimental spectra show that there is no other phase in the composite samples, except for Y-type hexaferrite. The lattice parameters and cell volume of the samples were calculated from the following equations:

$$d_{hkl} = \frac{1}{\sqrt{4\frac{(h^2 + hk + k^2)}{3a^2} + \frac{l^2}{c^2}}} \quad (1)$$

$$V_{cell} = \frac{\sqrt{3}}{2} a^2 c \quad (2)$$

where d_{hkl} is the d-spacing of the lines in the XRD pattern, and h, k and l are the corresponding Miller indices. The X-ray diffraction parameters and cell volume of $Sr_2Cu_{2-x}Co_xFe_{12}O_{22}$ (x = 0.0 to 1.0) are listed in Table 7. It is clear from Table 7 that there is not much change in value of lattice constants (a and c) as cobalt content increases, which may be due to almost equal ionic radii of Cu^{2+} (0.73 Å) and Co^{2+} (0.70 Å).

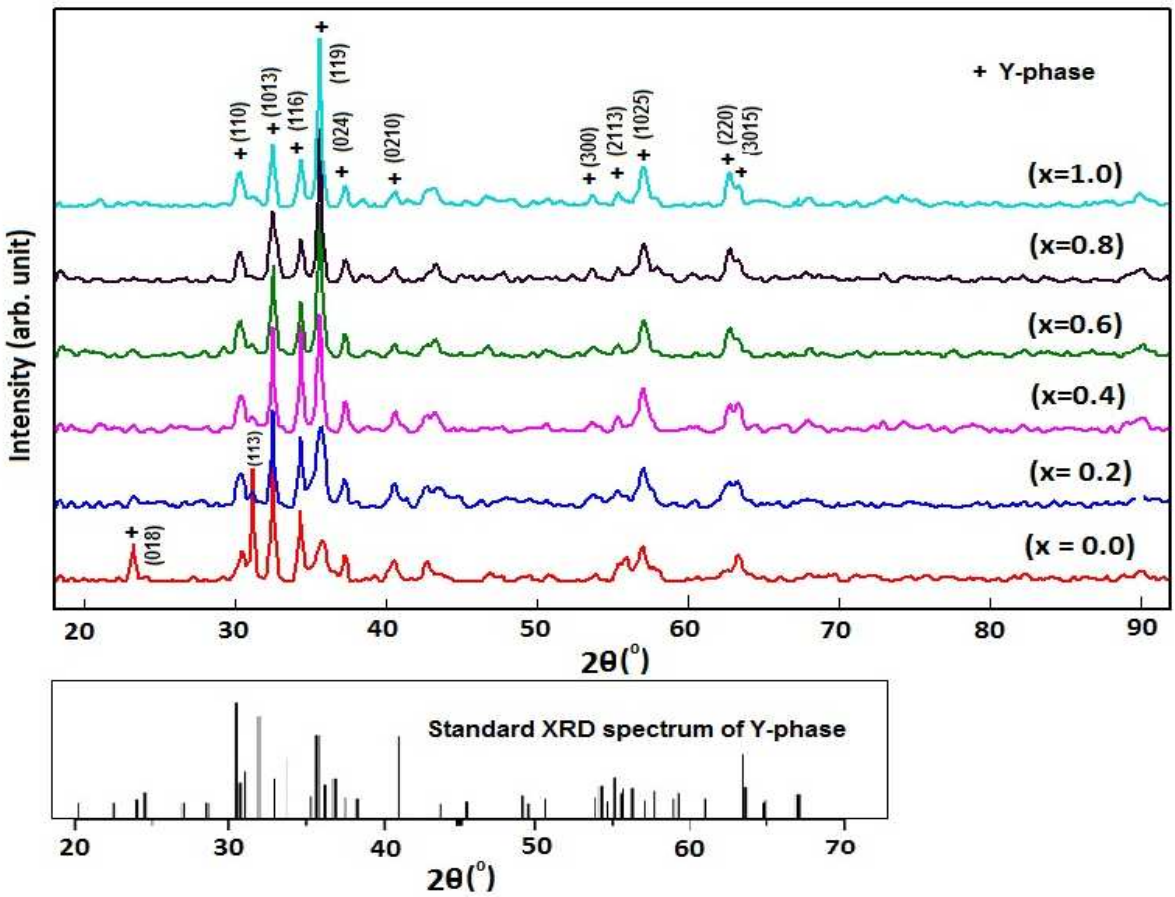

Fig. 9 X-ray diffraction pattern of $Sr_2Cu_{2-x}Co_xFe_{12}O_{22}$ (x = 0.0 to 1.0).

Table 7 Lattice constants (*a, c* and *a/c*), cell volume (*V cell*)

Sr. No	contents x	Lattice parameters a (Å)	c (Å)	c/a	Cell volume V (Å^3)
1	0.0	5.88	43.52	7.40	1301.98
2	0.2	5.89	43.52	7.39	1307.30
3	0.4	5.90	43.55	7.38	1311.31
4	0.6	6.20	43.59	7.03	1449.39
5	0.8	6.45	43.60	6.76	1568.99
6	1.0	6.45	43.62	6.76	1572.15

3.2.2 DSC analysis. DSC curves of dried precursors are recorded using a differential scanning calorimeter, model no. DSC-60, with a rate of 10 °C/min.To have a more clear understanding of $Sr_2Cu_{2-x}Co_xFe_{12}O_{22}$ forming mechanism from the solid precursors obtained after co-precipitation, the samples (x=0.2 to 0.8) were thermally analysed between temperature range of 25 °C to 350 °C and the resultant DSC curves are shown in Fig. 10 (b-e). The x=0.0 sample was thermally analysed between temperature range 20 °C to 150 °C (Fig. 10 (a)). During heat treatment of the precursors, several processes such as dehydration, oxidation of the residual organic groups, decomposition and sintering took place. A sharp exothermic peak is observed at 100°C in x=0.0 sample, which is due to the evaparation of absorbed water in the present sample. Between 115 °C to 350 °C, the samples (x=0.2 to 0.8) experienced strong endothermic and exothermic changes mainly attributed to the decomposition and oxidation of organic substances (Fig.10 (b) to (e)) [94, 96-98].

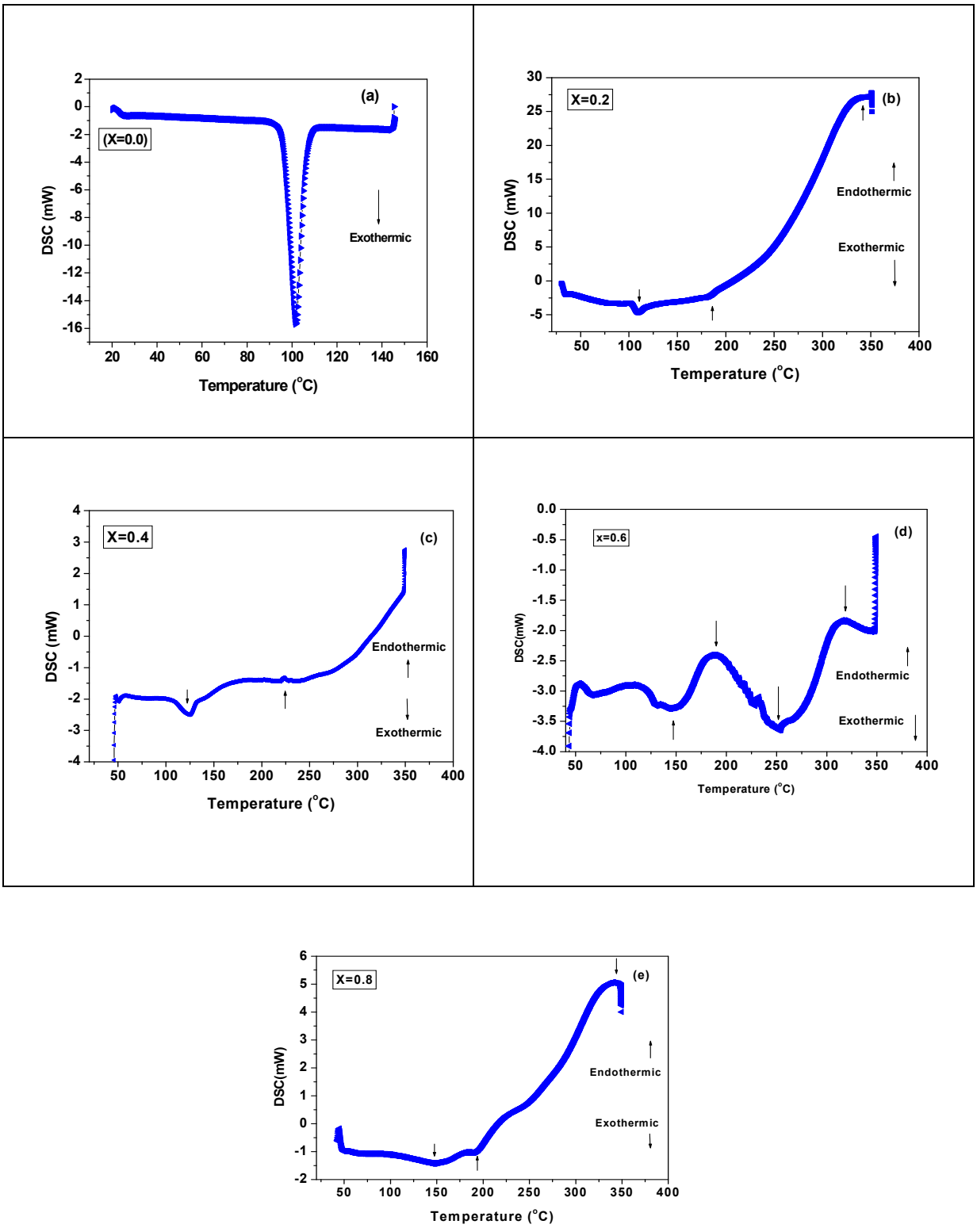

Fig. 10 (a-e) DSC curves of $Sr_2Cu_{2-x}Co_xFe_{12}O_{22}$ (x = 0.0 to 0.8).

3.2.3 FTIR analysis. The Fourier transform infrared (FTIR) spectra of $Sr_2Cu_{2-x}Co_xFe_{12}O_{22;}$ (x=0.2, 0.4, 0.6, 0.8) hexaferrite samples calcined at 950 °C were recorded at room temperature in wave number range from 4000 cm^{-1} to 400 cm^{-1} by using the KBr pallet method on FTIR Bruker Tenser 27 model. The FTIR spectra of raw and calcined samples are shown in Fig. 11. The absorption bands between 580 cm^{-1} to 440 cm^{-1} are observed in all calcined samples, which are due to Fe-O stretching and attributed to the formation of hexaferrite [94, 99,100].

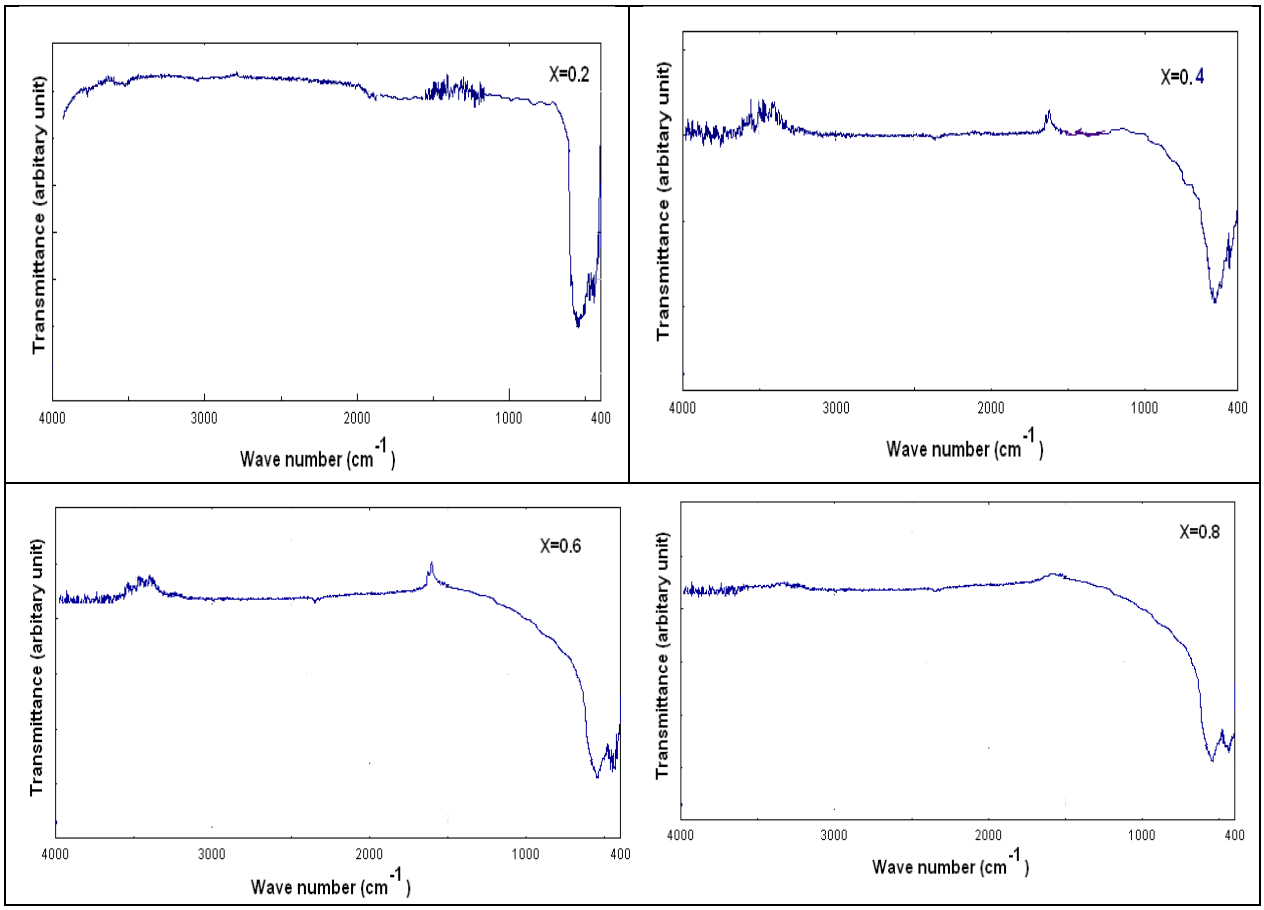

Fig. 11 FTIR Spectra of $Sr_2Cu_{2-x}Co_xFe_{12}O_{22}$ (x=0.2 to 0.8) samples.

3.4 SEM analysis. Scanning electron micrographs of prepared hexaferrite samples were obtained using a MAKE-LEO/LICA Model STEROECAN 440 scanning electron microscope. Figure 12 shows SEM micrographs of $Sr_2Cu_{2-x}Co_xFe_{12}O_{22}$ (x = 0.0 to 1.0) hexaferrite calcined powder, which were obtained after gold sputtering. A random distribution of micron to nanosized particles and agglomerations can be seen in the micrographs. We think that an attractive force existing between the molecules of strontium and ferric ions may lead to a surface inhomogeneity in the sample prepared using co-precipitation technique. Similar results have been observed for $BaFe_{12}O_{19}$ and $BaMg_2Fe_{10}O_{19}$ hexaferrite powders obtained by co-precipitation technique in our laboratory recently [101-103]. The major portion of particles size is in the range of 1 μm. Particle size was observed to increase with cobalt content (from x=0.0 to x=0.4). For x $\geq$0.6, small as well as large particles of different sizes and shapes are shown in SEM micrographs. It is clear from SEM micrographs that formed hexaferrite particles are well agglomerated to form the clusters of different sizes and shapes. The particles are found to be nonporous in nature. One may conclude that the cobalt composition plays a very crucial role in controlling the morphology of hexaferrite samples [104].

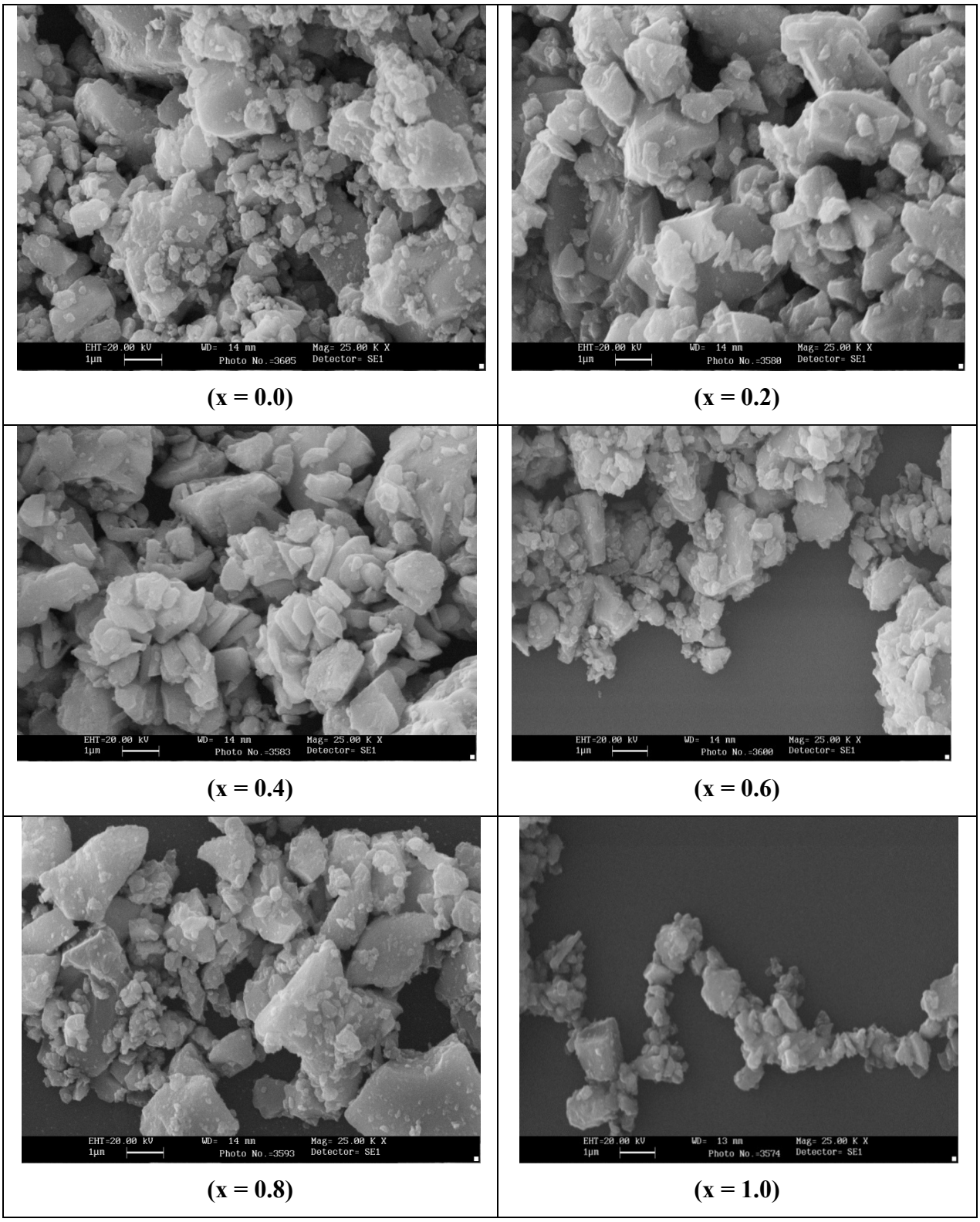

Fig. 12 SEM micrographs of $Sr_2Cu_{2-x}Co_xFe_{12}O_{22}$ (x = 0.0 to 1.0) hexaferrite samples.

4. Dielectric Properties

The ferrite powder was pressed at a pressure of 5 tons to obtain pellets of 1 cm diameter and 1.5 cm thickness. Polyvinyl alcohol (2% by weight) was used as binder. The pellets were sintered at 150° C for 2 h at a heating rate 150° C/h and subsequently furnace cooled. For dielectric measurement, silver paste was coated on polished surfaces of pellets to provide good electric contact.

The dielectric measurements were carried out over the frequency range of 100 Hz to 2 MHz at room temperature using an Agilent Precision LCR meter (Model No. E4980A). Dielectric constants were calaculated from the capacitance measurements. The variation of real dielectric constant (ε') and dielectric loss (tan δ) with frequency for $Sr_2Cu_{2-x}Co_xFe_{12}O_{22}$ (x = 0.0, 0.2, 0.4, 0.6, 0.8) hexaferrite samples are shown in Fig. 13 (a) and Fig. 13 (b), respectively.

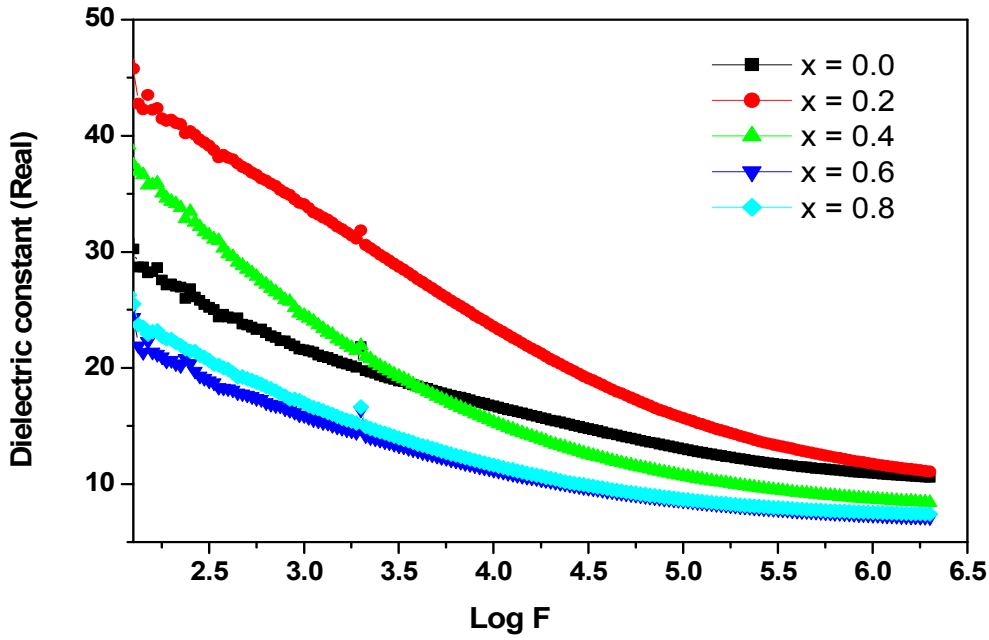

Fig. 13 (a) The variation of dielectric constant with log frequency at room temperature.

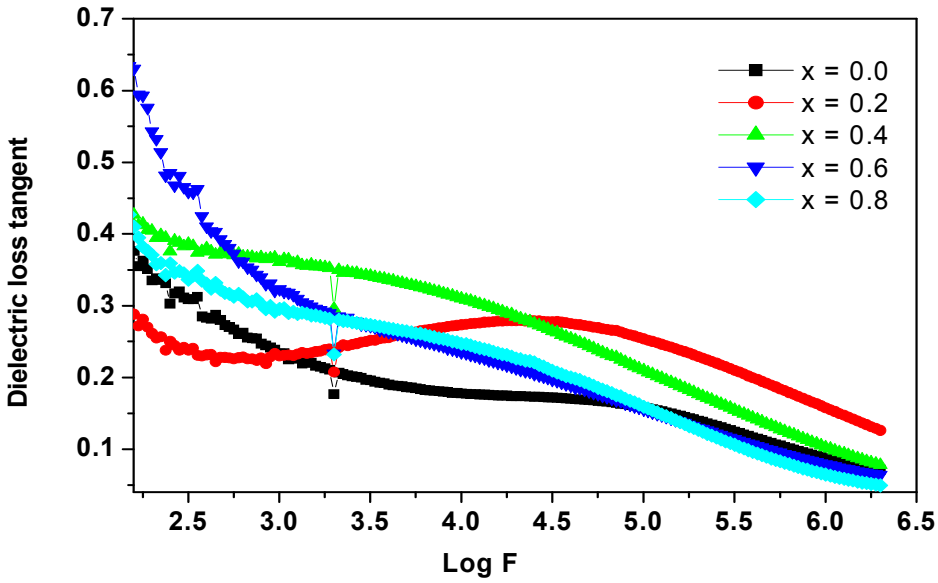

Fig. 13 (b) The variation of dielectric loss tangent with log frequency at room temperature.

The dielectric constant of the synthesized samples is calculated using the following equation:

$$C = \varepsilon_0 \varepsilon' (A/t) \quad (3)$$

where ε_0= dielectric permittivity in space (8.854 x 10^{-14} Farad/ cm), C = capacitance , A= area of circular face in cm^2.

The dielectric loss tangent (tan δ**)** can be expressed in terms of the real (**ε'**) and imaginary (ε **"**) parts of the dielectric constant as,

$$\tan \delta = (\varepsilon'')/(\varepsilon') \quad (4)$$

It is clear from Figures 13 (a) that the dielectric constant (Ɛ') decreases with increasing measuring frequency. This decrease in behaviour of (Ɛ') with frequency can be explained on the basis of the assumption that the phenomenon of the polarization process occurs in ferrites.The behaviour of dielectric loss tangent (tan δ) with log of frequency shows dielectric relaxation peaks, which shift towards lower frequencies with increasing cobalt content (x). This may be due to the existence of another peak lying at high frequencies beyond this frequency range. The appearance of the peaks in tan (δ) versus log frequency curve can be explained on the basis of the previous assumption of the polarization process [105].

Table 8 The variation of dielectric constant and loss tangent with frequency

x	f = 100 Hz		f = 1 KHz		f = 10 KHz		f = 1 MHz		f = 2 MHz	
	(Ɛ')	tan δ	(Ɛ')	tan δ	(Ɛ')	tan δ	(Ɛ')	tan δ	(Ɛ')	tan δ
0.0	13.24	1.129	21.54	0.233	16.71	0.177	10.91	0.087	10.57	0.071
0.2	32.85	0.301	34.10	0.229	23.55	0.273	11.73	0.157	11.05	0.126
0.4	29.13	0.887	24.48	0.361	15.33	0.310	8.69	0.102	8.40	0.078
0.6	20.10	0.696	15.90	0.323	11.19,	0.235	7.31	0.079	7.11	0.064
0.8	19.81	1.002	16.96	0.296	11.62	0.246	7.55	0.064	7.40	0.049

5. Magnetic Properties

The magnetic properties of $Sr_2Cu_{2-x}Co_xFe_{12}O_{22}$ (x = 0.0 to 0.8) hexaferrite samples were investigated using VSM on an EG&G Princeton Applied Research instrument (Model 4500). The magnetization curves of $Sr_2Cu_{2-x}Co_xFe_{12}O_{22}$ (x = 0.0 to 0.8) hexaferrite samples were measured on a VSM at room temperature under an applied field of 15 kOe. The initial magnetization and magnetic hysteresis curves of the samples calcined at 950 °C, recorded at room temperature, are shown in Fig. 14 (a) and 14 (b), respectively, and the magnetic parameters are listed in Table 9. The virgin curve lies completely inside the hysteresis loop. The saturation magnetization (Ms), as well as remanent magnetization (Mr), has been found to decrease with the cobalt doping. Similar result has been obtained for cobalt doped γ-Fe_2O_3 nanoparticles synthesized by the wet chemical method [106]. The value of ratio (Mr/Ms) of about 0.5 confirms that $Sr_2Cu_{2-x}Co_xFe_{12}O_{22}$ (x = 0.0 to 0.8) hexaferrite powder of single domain is produced [107].

Table 9 Magnetic parameters of $Sr_2Cu_{2-x}Co_xFe_{12}O_{22}$ (x = 0.0 to 0.8) hexaferrite powder (saturation magnetization—Ms and remanent magnetization—Mr)

Sr. No.	Cobalt content (x)	Mr	Ms	Mr/Ms
1	0.0	27.50	60.10	0.457
2	0.2	15.20	31.40	0.484
3	0.4	13.23	24.89	0.531
4	0.6	9.80	20.00	0.490
5	0.8	8.90	18.03	0.486

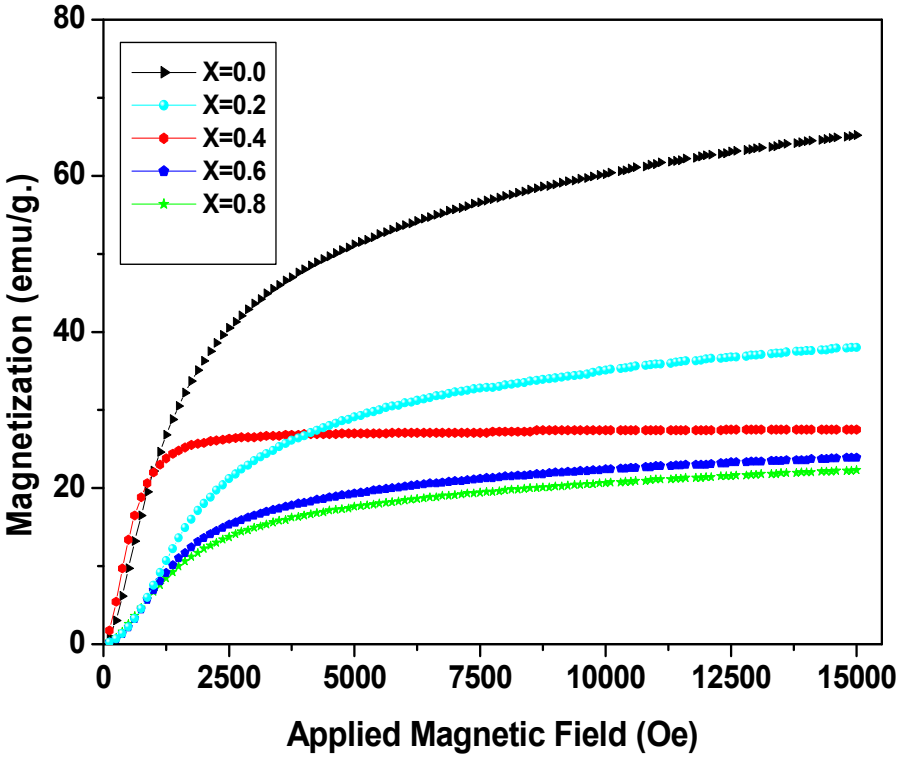

Fig. 14 (a) Initial magnetization curves of $Sr_2Cu_{2-x}Co_xFe_{12}O_{22}$ samples calcined at 950 °C, measured at RT.

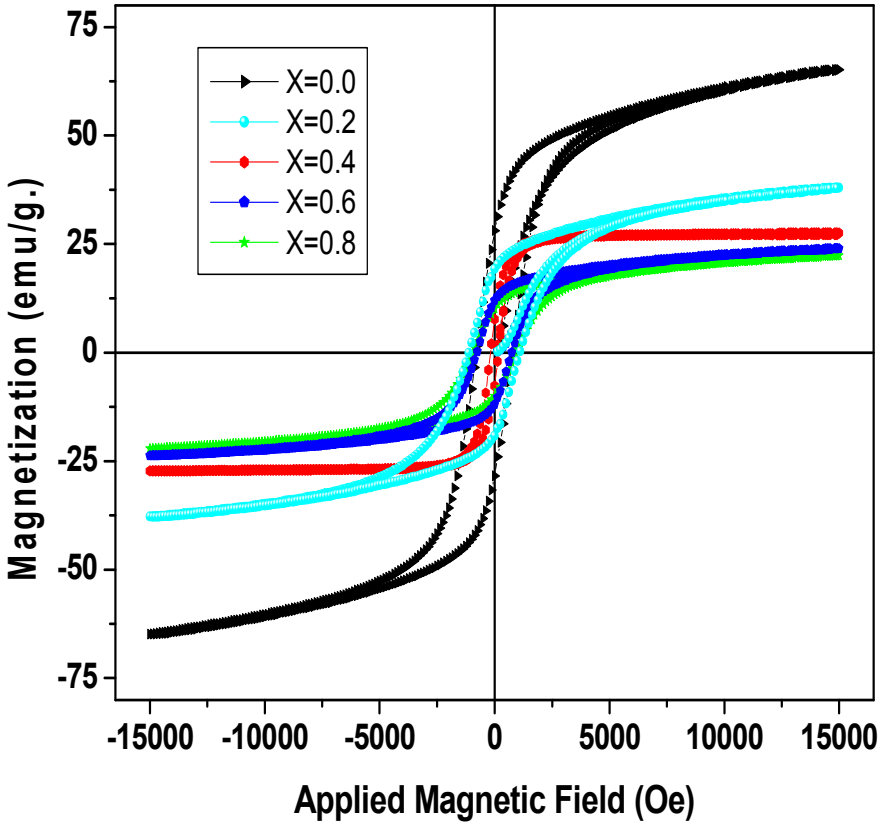

Fig. 14 (b) Hysteresis loops of $Sr_2Cu_{2-x}Co_xFe_{12}O_{22}$ samples calcined at 950 °C, measured at RT.

To look for the multiferroic signature of Y-type hexaferrites, magnetic properties were further investigated using a SQUID magnetometer (Cryogenic S600) in temperature range from 30K to 200K. The sample is initially cooled in a zero field to 30 K. Magnetic field of 15kOe is then applied and magnetization is recorded as the temperature is increased. This curve is called as zero-field cool (ZFC). A maximum magnetization is observed at temperature called T_b (blocking temperature). When the temperature reaches 200 K, the sample is progressively cooled and the magnetization is recorded. This curve is called field-cooled (FC). Fig 15 (a-e) shows ZFC/FC curves of $Sr_2Cu_{2-x}Co_xFe_{12}O_{22}$ samples calcined at 950 °C. Below temperature T_b, the particles are in a ferromagnetic state with an irreversible magnetization, whereas above this temperature, the magnetization is reversible and the particles are characterized by super paramagnetic behaviour [108,109]. Blocking temperature of x=0.6 sample is 36K, while the values for x=0.8 and x=1.0 samples are 42K and 49K, respectively. No clear cut signal for multiferroic character of Y-type hexaferrite has been detected in our investigations. Wang et al. [110] have reported in a recent publication their findings on the magnetically tunable ferroelectricity and giant magnetoelectric sensitivity up to 250 K in a Y-type hexaferrite, $BaSrCoZnFe_{11}AlO_{22}$. We hope to achieve the target by changing the composition of our Y-type hexaferrite in future investigations.

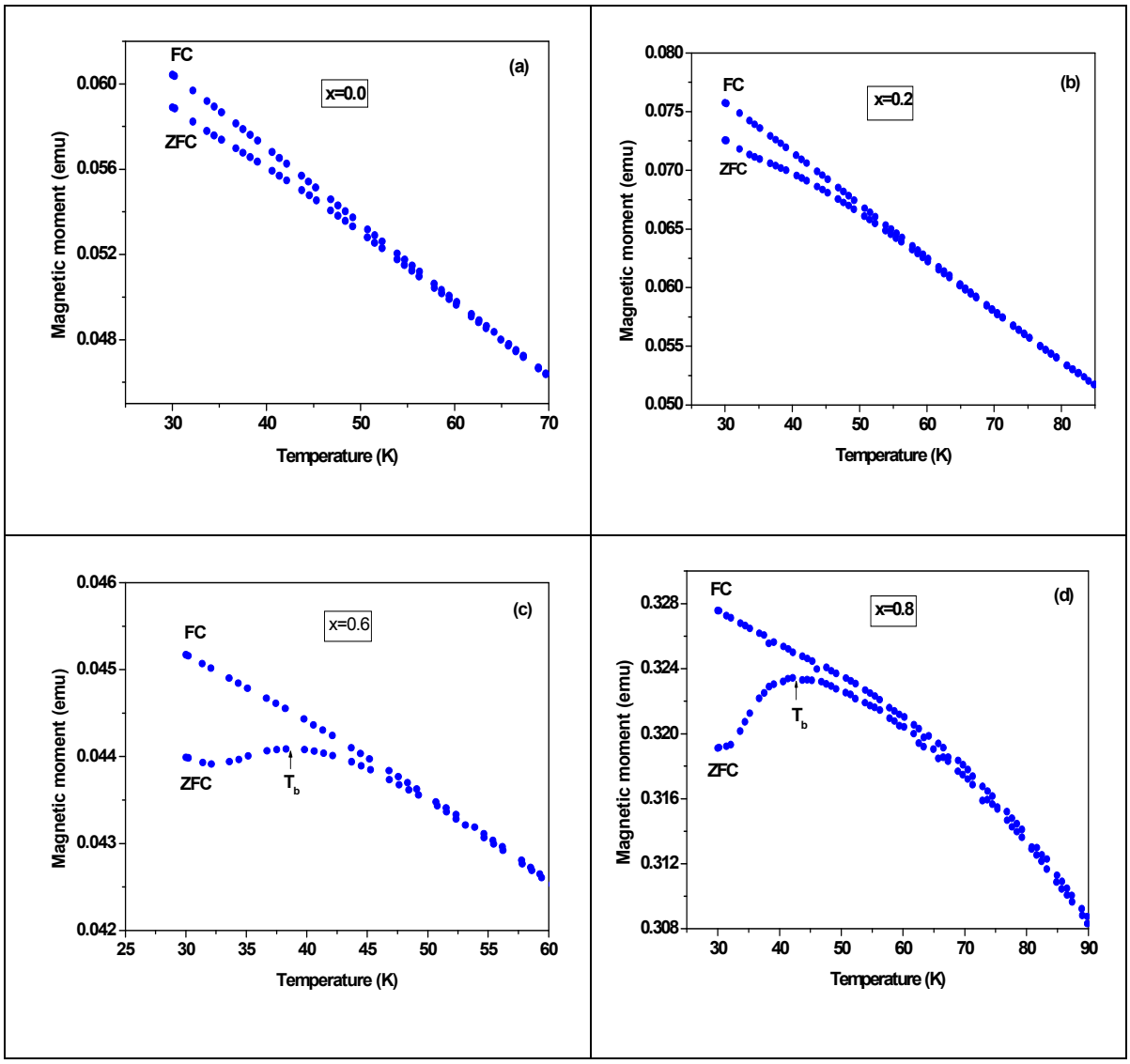

Fig. 15 (a,d) ZFC/FC curves of $Sr_2Cu_{2-x}Co_xFe_{12}O_{22}$ (x=0.0, 0.2, 0.6 and 0.8) samples calcined at 950 °C. The arrow indicates the transition between the ferromagnetic state (irreversible magnetization) and the super paramagnetic state (reversible magnetization with temperature).

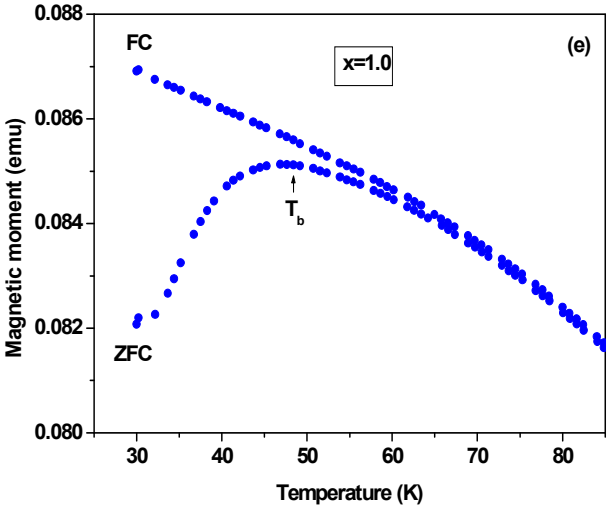

Fig. 15 (e) ZFC/FC curves of $Sr_2Cu_{2-x}Co_xFe_{12}O_{22}$ (x=1.0) sample calcined at 950 °C. The arrow indicates the transition between the ferromagnetic state (irreversible magnetization) and the super paramagnetic state (reversible magnetization with temperature).

6. Summary

This review is focused on the historical development of six different types of hexaferrites, their composition, structure and practical applications in diverse fields. Cobalt doped Y-type $Sr_2Cu_{2-x}Co_xFe_{12}O_{22}$, (x=0.0 to 1.0) hexaferrites have been investigated in detail. Cobalt doped Y-type hexaferrite particles have been synthesized using an aqueous co-precipitation chemical synthesis method followed by a single-step sintering at 950^o C. Optimized materials were characterized for structure, morphology, magnetic and dielectric properties using XRD, DSC, FTIR, SEM, VSM, SQUID and LCR bridge techniques. X-ray diffraction studies showed that sintering temperature as low as 950 ^{o} C was sufficient to produce a single-phase Y-type hexaferrite material. SEM analysis shows that the cobalt doping plays a very crucial role in controlling the morphology of hexaferrite samples. The dielectric (Ɛ') behaviour with frequency can be explained on the basis of the assumption that the phenomenon of the polarization process occurs in ferrites. The ratio (Mr/Ms) confirms that hexaferrite powder of single domain is produced. Low temperature magnetic measurements indicate that Y-type hexaferrite particles display a change from ferromagnetic state to super paramagnetic state at blocking temperature. The proposed synthesis approach may serve as a large-scale, cost-effective substitute to the conventional ceramic processing of hexagonal ferrite materials, which may also serve as potential multiferroics.

Acknowledgement

The experimental investigations reported in this review paper have been carried out under DRS-SAP program of UGC. Authors are thankful to Inter University Consortium (IUC), Indore for providing SQUID magnetometer facility.

References

[1] R. P. Feynman, R.B. Leighton and M. Sands: *The Feynman Lectures on Physics*, 2nd Ed., (Addison-Wesley, New York, 2005) Vol. 2, Chapter 34.
[2] G. W. Rathenau, J. Smit and A. L. Stuyts: Z. Phys. Vol. 133 (1952), p. 250.
[3] M. T. Weiss and P. W. Anderson: Phys. Rev. Vol. 98 (1955), p. 925.
[4] M. T. Weiss: IRE Conv. Rec. Vol. 3 (1955), p. 95.
[5] K. J. Sixtus, K. J. Kronenberg and R. K. Tenzer : J. Appl. Phys. Vol. 27 (1956), p. 1051.

[6] N. Matsushita, M. I. Chinose, S. Nagakawa and M. Naoe: IEEE Trans. Magn. Vol. 4 (1998), p. 1641.
[7] Y. Chen and M. H. Kryder: IEEE Trans. Magn. Vol. 34 (1998), p. 729.
[8] Y. Chen, D. E. Laughlin, X. Ma and M. H. Kryder: J. Appl. Phys. Vol. 81 (1997), p. 4380.
[9] A. Morisako, X. Liu and M. Matsumoto: J. Appl. Phys. Vol. 81 (1997), p. 4374.
[10] M. Y. Salunkhe and D. K. Kulkarni: J. Magn. Magn. Mater. Vol. 279 (2004), p. 64.
[11] A. Goldman: *Modern Ferrite Technology*, 2nd Ed. (Springer, New York 2006).
[12] J. Slama, A. Gruskova, V. Jancarik, M. Stofka and A. Gonzalez-Angeles: Acta Physica Polonica A. Vol. 113 (2008), p. 609.
[13] G. H. Jonker, H. P. Wijn and P. B. Braun: Philips. Technol. Rev. Vol. 18 (1956–57), p. 145.
[14] C. Sudakar, G. N. Subbanna and T. R. N. Kutty: J. Magn. Magn. Mater. Vol. 268 (2004), p. 75.
[15] D. Lisjak and M. Drofenik: J. Am. Ceram. Soc. Vol. 90 (2007), p. 3517.
[16] M. Pieper, A. Moreland and F. Kools: J. Magn. Magn. Mater. Vol. 242 (2002), p. 1408.
[17] A. Morel, J. M. Le Breton, J. Kreisel, G. Wiesinger, F. Kools and P. Tenaud: J. Magn. Magn. Mater. Vol. 242 (2002), p. 1405.
[18] A. Collomb, B. Lambert Andron, J. X. Boucherle and D. Samaras: Phys. Stat. Sol. (A) Vol. 96 (1986), p. 385.
[19] J. Smit and H. P. J. Wijn: *Ferrites* (Philips Technical Library, Eindhoven, The Netherlands, 1959)
[20] L. Lechevallier, J. M. L. Breton, J. F. Wang and I. R. Harris: J. Magn. Magn. Mater. Vol. 269 (2004), p. 192.
[21] M. Pardavi-Horvath: J. Magn. Magn. Mater. Vol. 216 (2000), p. 171.
[22] V. G. Harris, A. Geiler, Y. Chen, S. D. Yoon, M. Z. Wu, A. Yang, Z. Chen, P. He, P. V. Parimi, X. Zuo, C. E. Patton , M. Abe, O. Acher and C. Vittoria: J. Magn. Magn. Mater. Vol. 321 (2009), p. 2035.
[23] Z. D. Han, L. M. Dong, Z. Wu, L. W. Shan and X. Y. Zhang: Key Eng. Mater. Vol. 336– 338 (2007), p. 688.
[24] V. G. Harris: J. Appl. Phys. Vol. 99 (2006), p. 08M911.
[25] B. Lax and K. J. Button: *Microwave Ferrites and Ferrimagnetics* (McGraw-Hill, New York 1962).
[26] W. H.von Aulock: *Handbook of Microwave Ferrite Materials* (Academic Press, New York 1965).
[27] Ü. Özgüri, Y. Alivov and H. Morkoç: *Microwave Ferrites, Part 1: Fundamentals and self biasing,* J. Mater. Sci. Vol. 20 (2009) p. 789
[28] F. K. Lotgering, P. H. G. M. Vromans and M. A. H. Huybens: J. Appl. Phys. Vol. 51 (1980), p. 5913.
[29] N. Rezlescu and C. Rezlescu: Phys. Stat. Sol. (A) Vol. 23 (1974), p. 575.
[30] F. Leccabue, R. Panizzieri and G. Salvaiti: J. Appl. Phys. Vol. 59 (1986), p. 2114.
[31] A. Paoluzi, F. Licci, O. Moze, G. Turilli, A. Deriu, G. Albanese and E. Calabrese: J. Appl. Phys. Vol. 63 (1988), p. 5074.
[32] R. B. Jotania, R. B. Khomane, C. C. Chauhan, S. K. Menon and B. D. Kulkarni: J. Magn. Magn. Mater. Vol. 320 (2008), p. 1095.
[33] A. M. Abo El Ata and M. A. Ahmed: J. Magn. Magn. Mater. Vol. 208 (2000), p. 27.
[34] Z. W. Li, L. F. Chen, Y. P. Wu and C. K. Ong: J. Appl. Phys. Vol. 96 (2004), p. 534.
[35] H. Kojima, in: *Ferromagnetic Materials*: *A Handbook on the Properties of Magnetically Ordered Substances,* edited by E. P. Wohlfarth (North-Holland, Amsterdam, 1982), Vol. 3, Chap. 5, p. 305–391
[36] M. A. Ahmed, N. Okasha and R. M. Kershi: Mater. Chem. Phys. Vol. 113 (2009), p. 196.
[37] Y. P. Wu, C. K. Ong, G. Q. Lin and Z. W. Li: J. Phys. D: Appl. Phys. Vol. 39 (2006), p. 2915.

[38] W. Z. Li, Y. P. Wu, G. Q. Lin and T. Liu: IEEE Trans. Magn. Vol. 42 (2006), p. 3365.
[39] J. D. Adam, L. E. Davis, G. F. Dionne, E. F. Schloemann and S. N. Stitzer : IEEE Trans. Microwave Theory Tech. Vol. (2002), p. 721.
[40] Y. P. Wu, C. K. Ong, Z. W. Li, L. Chen, G. Q. Lin and S. J. Wang: J. Appl. Phys. Vol. 97 (2005), p. 063909.
[41] R. C. Puller, S. G. Appleton and A. K. Bhattacharya: J. Mat. Sci. Lett. Vol.17 (1998), p. 973.
[42] X. H. Wang, T.L. Ren and L.Y. Li: J. Magn. Magn. Mater. Vol. 184 (1998), p. 95.
[43] M. El-Saadawy: J. Magn. Magn. Mater. Vol. 219 (2000), p. 69.
[44] S. P. Ruan, B. K. Xu and H. Suo, J. Magn. Magn. Mater. Vol. 212 (2000), p. 175.
[45] G. Asti, F. Bolzoni, F. Licci and M. Canali: IEEE Trans. Magn. Vol. 14 (1978), p. 883.
[46] G. Albanese, E. Calabrese, A. Deriu and F. Licci: Hyperfine Interact. Vol. 28 (1986), p. 487.
[47] A. Paoluzi, F. Licci, O. Moze, G. Turilli, A. Deriu, G. Albanese and E. Calabrese: J. Appl. Phys. Vol. 63 (1988), p. 5074.
[48] D. Samaras, A. Collomb, S. Hadjivasiliou, C. Achilleos, J. Tsoukalas, J. Pannetier and J. Rodriguez: J. Magn. Magn. Mater. Vol. 79 (1989), p. 193.
[49] E. P. Naiden, V. I. Maltsev and G. I. Ryabtsev: Phys. Stat. Sol. (A) Vol. 120 (1990), p. 209.
[50] E. P. Naiden and G. I. Ryabtsev: Russ. Phys. J. Vol. 33 (1990), p. 318.
[51] C. Sürig, K. A. Hempel, R. Müller and P. Görnert: J. Magn. Magn. Mater. Vol. 150 (1995), p. 269.
[52] G. Turilli and G. Asti: J. Magn. Magn. Mater. Vol. 157–158 (1996), p. 371.
[53] E. P. Naiden and S. M. Zhilyakov: Russ. Phys. J. Vol. 40 (1997), p. 869.
[54] G. Albanese, M. Carbucicchio and G. Asti: Appl. Phys. Vol. 11 (1976), p. 81.
[55] A. P. Lilot, A. Gerard and F. Grandjean: IEEE Trans. Magn. Mag. Vol. 18 (1982), p. 1463.
[56] J. Smit, H. P. J. Wijin: *Ferrites, Physical Properties of Ferromagnetic Oxides in Relation to Their Technical Applications* (Wiley, Netherlands 1959).
[57] L. D. Xin, Z. N. Nin, G. S. Jiao, L. G. Dong and W. H. Zong: IEEE Trans. Magn. Vol. 25 (1989), p. 3290.
[58] E. J. Verwey, P. W. Haaijam, F. C. Romeyn and G. W. Van Oosterhout: Philips Res. Rep. Vol. 5 (1950), p. 173.
[59] P. B. Braun : Philips Res. Rep. Vol.12 (1957), p. 491.
[60] F. Leccabue, R. Panizzieri, G. Bocelli , G. Calestani , C. Rizzoli and N. S. Almodovar: J. Magn. Magn. Mater Vol. 68 (1987), p. 365.
[61] Z. Haijun, Y. Xi and Z. Liangying: J. Magn. Magn. Mater. Vol. 241 (2002), p. 441.
[62] K. Taniguchi, N. Abe1, S. Ohtani1, H. Umetsu1 and T. Arima: Appl. Phys. Express Vol. 1 (2008), p. 031301.
[63] S. Ishiwata,Y. Taguchi, H. Murakawa, Y. Onose and Y. Tokura: Science Vol. 319 (2008), p. 1643.
[64] T. Kimura, G. Lawes and A.P. Ramirez: Phys. Rev. Lett. Vol. 94 (2005), p. 137201.
[65] S. Ishiwata, Y. Taguchi, Y. Tokunaga, H. Murakawa,Y. Onose and Y. Tokura: Phy Rev. B Vol. 79 (2009), p. 180408.
[66] Y. Bai, J. Zhou, Z. Gui and L. Li : Mater. Chem. Phys. Vol. 98 (2006), p. 66.
[67] M. Obol, X. Zuo and C. Vittoria: J. Appl. Phys. Vol. 91 (2006), p. 7616.
[68] T. Nakamura and K. I. Hatakeyama: IEEE Trans. Magn. Vol.36 (2000), p. 3415.
[69] H. J. Kwon, J. Y. Shin and J. Y. Oh: J. Appl. Phys. Vol. 75, (1994), p. 6109.
[70] M. Obol and C. Vittoria: J. Appl. Phys. Vol. 94 (2003), p. 4013.
[71] M. Obol and C. Vittoria: IEEE Trans. Magn. Vol. 39 (2003), p. 3103.
[72] M. Obol and C. Vittoria: J. Magn. Magn. Mater. Vol. 272–276, (2004), p. E1799.
[73] M. Obol and C. Vittoria, J. Magn. Magn. Mater. Vol. 265 (2003), p. 290.
[74] Y. Bai, J. Zhou, Z. Gui and L. Li: J. Magn. Magn. Mater. Vol. 250 (2002), p. 364.
[75] G. Albanese: Journal de Physique, *Colloque* CI, Vol. 38 (1977), p. Cl-85.

[76] Y. Kitagawa, Y. Hiraoka, T. Honda, T. Ishikura, H. Nakamura and T. Kimura: Nature Mater. Vol. 9 (2010), p. 797.
[77] A. Elkady, M.M. Abou-Sekkina and K. Nagorny: Hyperfine Interact. Vol. 128 (2000), p. 423.
[78] H. Zhang, J. Zhou j, Z. Yue, P. Wu, Z. Gui and L. Li: Mater. Lett. Vol. 43 (2000), p. 62.
[79] Z. Wang, L. Li, S. Su, Z. Gui, Z. Yue and J. Zhou: J. Eur. Cer. Soc. Vol. 23 (2003), p. 715.
[80] A. J. Kerecman, A. Tauber, T. R. Aucoin and R. O. Savage: J. Appl. Phys. Vol. 39 (1968), p. 726.
[81] R. C. Pullar and A. K. Bhattacharya: J. Mater. Sci. Vol. 36 (2001), p. 4805.
[82] D. Lisjak, D. Makovec and M. Drofenik: J. Mater. Res. Vol.19 (2004), p. 2462.
[83] H. Jonker, H. P. Wijn and P. B. Braun: Philips Tech. Rev. Vol. 13 (1952), p. 194.
[84] A.J. Kerecman, A. Tauber and W. P. Dattilo: J. Appl. Phys. Vol. 40 (1969), p. 1416.
[85] E.P. Wohlfarth: *Ferromagnetic Materials* (North-Holland, Amaterdam 1982), p. 404.
[86] H. Zhang, Z. Liu, X. Yao, L. Zhang and M. Wu: Mater. Sci. Eng. B Vol. 97 (2003), p. 160.
[87] G. Albanese, A. Deriu, F. Licci and S. Rinaldi: IEEE Trans. Magn. Mag. Vol.14, (1978), p.710.
[88] A. Deriu, F. Licci, S. Rinaldi and T. Besagni: J. Magn. Magn. Mater. Vol. 22 (1981) p.257.
[89] S. G. Lee and S. J. Kwon: J. Magn. Magn. Mater. Vol. 153 (1996), p. 279.
[90] M. A. El Hiti and A. M. A. Abo El Ata: J. Magn. Magn. Mater. Vol. 195 (1999), p. 667.
[91] H. Sagayama, K. Taniguchi, N. Abe, T. Arima, Y. Nishikawa, S. Yano, Y. Kousaka, J. Akimitsu, M. Matsuura and K. Hirota: Phys. Rev. B Vol. 80 (2009). p. 180419-1-5.
[92] M. Nagae, T. Atsumi and T. Yoshio: J. Am. Ceram. Soc. Vol. 89 (2006), p. 1122.
[93] J. Jalli, Y. Hong, S. Bae, J. Lee, G. S. Abo, J. Park, B. Choi, T. Mewes, S. Kim, S. Gee, I.T. Nam and T. Tanaka: J. Appl. Phys. Vol. 109 (2011), p. 07A509
[94] J. Temuujin, M. Aoyama, M. Senna, T. Masuko, C. Ando and H. Kishi: J. Solid State. Chem. Vol. 177 (2004), p. 3903.
[95] X. Li, R. Gong, Z. Feng, J. Yan, X. Shen and H. He: J. Am. Ceram. Soc. Vol. 89 (2006), p. 1450.
[96] X. He, Q. Zhang and Z. Lang: Mater. Lett. Vol. 57 (2003), p. 3031.
[97] H. Y. He, J. F. Huang, L Y Cao, Z. He and Q. Shen**:** Bull. Mater. Sci. Vol. 34 (2011), p. 463.
[98] S. Nasir and M. Anis-ur-Rehman: Phys. Scr. Vol. 84 (2011), p. 025603.
[99] R. C. Pullar, M. D. Taylor and A. K. Bhattacharya: J. Mater. Sci. Vol. 32 (1997), p. 873.
[100] K. Maruszewski, D. P. Strommen and J. R. Kincaid: J. Am. Chem. Soc. Vol. 115 (1993), p. 8345.
[101] R. Jotania, C. Chauhan, S. Menon and K. Jotania: Adv. Mater. Res. Vol. 67 (2009) p. 137.
[102] H.S. Virk, P. Sharma and R. Jotania: Int. J. Adv. Eng. Tech. Vol. 2 (2011), p. 131.
[103] R. Jotania, P. Sharma and H.S. Virk:J. Nanosci. Lett. Vol. 1 (2011), p. 63.
[104] P. D. Popa, E. Rezlescu, C. Doroftei and N. Rezlescu: J. Optoelectron. Adv. Mater. Vol. 7 (2005), p. 1553.
[105] K. Iwavchi: J. Appl. Phys. Vol. 10 (1971), p. 1520.
[106] S. Chakrabarti, S. K. Mandal and S. Chaudhuri: Nanotechnology Vol. 16 (2005) p. 506.
[107] H. F.Yu and K. C. Huang: J. Magn. Magn. Mater. Vol. 260 (2003), p. 455.
[108] J. L. Dormann: Rev. Phys. Appl. Vol. 16 (1981), p. 275.
[109] E. Vincent, J. Hamann, P. Preno and E. Tronc: J. Phys. Chem. Vol. 4 (1994) p. 273.
[110] F. Wang, T. Zou, L.Q. Wan and Y. Sun: Appl. Phys. Lett. Vol. 100 (2012), p. 122901.

Ferroics and Multiferroics
10.4028/www.scientific.net/SSP.189

Y-Type Hexaferrites: Structural, Dielectric and Magnetic Properties
10.4028/www.scientific.net/SSP.189.209

DOI References
[2] G. W. Rathenau, J. Smit and A. L. Stuyts: Z. Phys. Vol. 133 (1952), p.250.
doi:10.1007/BF01948700
[5] K. J. Sixtus, K. J. Kronenberg and R. K. Tenzer : J. Appl. Phys. Vol. 27 (1956), p.1051.
doi:10.1063/1.1722540
[6] N. Matsushita, M. I. Chinose, S. Nagakawa and M. Naoe: IEEE Trans. Magn. Vol. 4 (1998), p.1641.
doi:10.1109/20.706641
[8] Y. Chen, D. E. Laughlin, X. Ma and M. H. Kryder: J. Appl. Phys. Vol. 81 (1997), p.4380.
doi:10.1063/1.364830
[9] A. Morisako, X. Liu and M. Matsumoto: J. Appl. Phys. Vol. 81 (1997), p.4374.
doi:10.1063/1.364828
[10] M. Y. Salunkhe and D. K. Kulkarni: J. Magn. Magn. Mater. Vol. 279 (2004), p.64.
doi:10.1016/j.jmmm.2004.01.046
[14] C. Sudakar, G. N. Subbanna and T. R. N. Kutty: J. Magn. Magn. Mater. Vol. 268 (2004), p.75.
doi:10.1016/S0304-8853(03)00476-1
[15] D. Lisjak and M. Drofenik: J. Am. Ceram. Soc. Vol. 90 (2007), p.3517.
doi:10.1016/j.jeurceramsoc.2007.02.202
[16] M. Pieper, A. Moreland and F. Kools: J. Magn. Magn. Mater. Vol. 242 (2002), p.1408.
doi:10.1016/S0304-8853(01)00963-5
[17] A. Morel, J. M. Le Breton, J. Kreisel, G. Wiesinger, F. Kools and P. Tenaud: J. Magn. Magn. Mater. Vol. 242 (2002), p.1405.
doi:10.1016/S0304-8853(01)00962-3
[18] A. Collomb, B. Lambert Andron, J. X. Boucherle and D. Samaras: Phys. Stat. Sol. (A) Vol. 96 (1986), p.385.
doi:10.1002/pssa.2210960203
[20] L. Lechevallier, J. M. L. Breton, J. F. Wang and I. R. Harris: J. Magn. Magn. Mater. Vol. 269 (2004), p.192.
doi:10.1016/S0304-8853(03)00591-2
[21] M. Pardavi-Horvath: J. Magn. Magn. Mater. Vol. 216 (2000), p.171.
doi:10.1016/S0304-8853(00)00106-2
[22] V. G. Harris, A. Geiler, Y. Chen, S. D. Yoon, M. Z. Wu, A. Yang, Z. Chen, P. He, P. V. Parimi, X. Zuo, C. E. Patton , M. Abe, O. Acher and C. Vittoria: J. Magn. Magn. Mater. Vol. 321 (2009), p. (2035).
doi:10.1016/j.jmmm.2009.01.004
[23] Z. D. Han, L. M. Dong, Z. Wu, L. W. Shan and X. Y. Zhang: Key Eng. Mater. Vol. 336– 338 (2007), p.688.
doi:10.4028/www.scientific.net/KEM.336-338.688
[28] F. K. Lotgering, P. H. G. M. Vromans and M. A. H. Huybens: J. Appl. Phys. Vol. 51 (1980), p.5913.

doi:10.1063/1.327493
[29] N. Rezlescu and C. Rezlescu: Phys. Stat. Sol. (A) Vol. 23 (1974), p.575.
doi:10.1002/pssa.2210230229
[30] F. Leccabue, R. Panizzieri and G. Salvaiti: J. Appl. Phys. Vol. 59 (1986), p.2114.
doi:10.1063/1.336400
[32] R. B. Jotania, R. B. Khomane, C. C. Chauhan, S. K. Menon and B. D. Kulkarni: J. Magn. Magn. Mater. Vol. 320 (2008), p.1095.
doi:10.1016/j.jmmm.2007.10.032
[33] A. M. Abo El Ata and M. A. Ahmed: J. Magn. Magn. Mater. Vol. 208 (2000), p.27.
doi:10.1016/S0304-8853(99)00547-8
[34] Z. W. Li, L. F. Chen, Y. P. Wu and C. K. Ong: J. Appl. Phys. Vol. 96 (2004), p.534.
doi:10.1088/0305-4470/37/7/015
[35] H. Kojima, in: Ferromagnetic Materials: A Handbook on the Properties of Magnetically Ordered Substances, edited by E. P. Wohlfarth (North-Holland, Amsterdam, 1982), Vol. 3, Chap. 5, p.305–391.
doi:10.1063/1.2914974
[36] M. A. Ahmed, N. Okasha and R. M. Kershi: Mater. Chem. Phys. Vol. 113 (2009), p.196.
doi:10.1016/j.matchemphys.2008.07.032
[39] J. D. Adam, L. E. Davis, G. F. Dionne, E. F. Schloemann and S. N. Stitzer : IEEE Trans. Microwave Theory Tech. Vol. (2002), p.721.
doi:10.1109/22.989957
[43] M. El-Saadawy: J. Magn. Magn. Mater. Vol. 219 (2000), p.69.
doi:10.1016/S0304-8853(00)00034-2
[44] S. P. Ruan, B. K. Xu and H. Suo, J. Magn. Magn. Mater. Vol. 212 (2000), p.175.
doi:10.1016/S0304-8853(99)00755-6
[45] G. Asti, F. Bolzoni, F. Licci and M. Canali: IEEE Trans. Magn. Vol. 14 (1978), p.883.
doi:10.1109/TMAG.1978.1059784
[46] G. Albanese, E. Calabrese, A. Deriu and F. Licci: Hyperfine Interact. Vol. 28 (1986), p.487.
doi:10.1007/BF02061493
[47] A. Paoluzi, F. Licci, O. Moze, G. Turilli, A. Deriu, G. Albanese and E. Calabrese: J. Appl. Phys. Vol. 63 (1988), p.5074.
doi:10.1063/1.340405
[48] D. Samaras, A. Collomb, S. Hadjivasiliou, C. Achilleos, J. Tsoukalas, J. Pannetier and J. Rodriguez: J. Magn. Magn. Mater. Vol. 79 (1989), p.193.
doi:10.1016/0304-8853(89)90098-X
[49] E. P. Naiden, V. I. Maltsev and G. I. Ryabtsev: Phys. Stat. Sol. (A) Vol. 120 (1990), p.209.
doi:10.1002/pssa.2211200119
[50] E. P. Naiden and G. I. Ryabtsev: Russ. Phys. J. Vol. 33 (1990), p.318.
doi:10.1007/BF00894211
[52] G. Turilli and G. Asti: J. Magn. Magn. Mater. Vol. 157–158 (1996), p.371.
doi:10.1016/0304-8853(95)01260-5
[53] E. P. Naiden and S. M. Zhilyakov: Russ. Phys. J. Vol. 40 (1997), p.869.
doi:10.1134/1.1130010
[54] G. Albanese, M. Carbucicchio and G. Asti: Appl. Phys. Vol. 11 (1976), p.81.
doi:10.1007/BF00895020

[55] A. P. Lilot, A. Gerard and F. Grandjean: IEEE Trans. Magn. Mag. Vol. 18 (1982), p.1463.
doi:10.1109/TMAG.1982.1062044
[60] F. Leccabue, R. Panizzieri, G. Bocelli , G. Calestani , C. Rizzoli and N. S. Almodovar: J. Magn. Magn. Mater Vol. 68 (1987), p.365.
doi:10.1016/0304-8853(87)90015-1
[61] Z. Haijun, Y. Xi and Z. Liangying: J. Magn. Magn. Mater. Vol. 241 (2002), p.441.
doi:10.1016/S0304-8853(01)00447-4
[65] S. Ishiwata, Y. Taguchi, Y. Tokunaga, H. Murakawa,Y. Onose and Y. Tokura: Phy Rev. B Vol. 79 (2009), p.180408.
doi:10.1103/PhysRevB.79.180408
[68] T. Nakamura and K. I. Hatakeyama: IEEE Trans. Magn. Vol. 36 (2000), p.3415.
doi:10.1109/20.908844
[70] M. Obol and C. Vittoria: J. Appl. Phys. Vol. 94 (2003), p.4013.
doi:10.1109/MWSYM.2003.1210968
[71] M. Obol and C. Vittoria: IEEE Trans. Magn. Vol. 39 (2003), p.3103.
doi:10.1109/MWSYM.2003.1210968
[72] M. Obol and C. Vittoria: J. Magn. Magn. Mater. Vol. 272–276, (2004), p. E1799.
doi:10.1016/j.jmmm.2003.12.1116
[73] M. Obol and C. Vittoria, J. Magn. Magn. Mater. Vol. 265 (2003), p.290.
doi:10.1016/S0304-8853(03)00277-4
[76] Y. Kitagawa, Y. Hiraoka, T. Honda, T. Ishikura, H. Nakamura and T. Kimura: Nature Mater. Vol. 9 (2010), p.797.
doi:10.1038/nmat2826
[77] A. Elkady, M.M. Abou-Sekkina and K. Nagorny: Hyperfine Interact. Vol. 128 (2000), p.423.
doi:10.1023/A:1012612405813
[78] H. Zhang, J. Zhou j, Z. Yue, P. Wu, Z. Gui and L. Li: Mater. Lett. Vol. 43 (2000), p.62.
doi:10.1016/S0167-577X(99)00231-1
[79] Z. Wang, L. Li, S. Su, Z. Gui, Z. Yue and J. Zhou: J. Eur. Cer. Soc. Vol. 23 (2003), p.715.
doi:10.1016/S0955-2219(02)00157-7
[80] A. J. Kerecman, A. Tauber, T. R. Aucoin and R. O. Savage: J. Appl. Phys. Vol. 39 (1968), p.726.
doi:10.1063/1.2163602
[81] R. C. Pullar and A. K. Bhattacharya: J. Mater. Sci. Vol. 36 (2001), p.4805.
doi:10.1023/A:1017947625940
[82] D. Lisjak, D. Makovec and M. Drofenik: J. Mater. Res. Vol. 19 (2004), p.2462.
doi:10.1557/JMR.2004.0317
[84] A.J. Kerecman, A. Tauber and W. P. Dattilo: J. Appl. Phys. Vol. 40 (1969), p.1416.
doi:10.1063/1.1657698
[87] G. Albanese, A. Deriu, F. Licci and S. Rinaldi: IEEE Trans. Magn. Mag. Vol. 14, (1978), p.710.
doi:10.1109/TMAG.1978.1059812
[88] A. Deriu, F. Licci, S. Rinaldi and T. Besagni: J. Magn. Magn. Mater. Vol. 22 (1981) p.257.
doi:10.1016/0304-8853(81)90030-5
[90] M. A. El Hiti and A. M. A. Abo El Ata: J. Magn. Magn. Mater. Vol. 195 (1999), p.667.
doi:10.1016/S0304-8853(99)00120-1
[91] H. Sagayama, K. Taniguchi, N. Abe, T. Arima, Y. Nishikawa, S. Yano, Y. Kousaka, J. Akimitsu, M.

Matsuura and K. Hirota: Phys. Rev. B Vol. 80 (2009). pp.180419-5.
doi:10.1103/PhysRevB.80.180419
[92] M. Nagae, T. Atsumi and T. Yoshio: J. Am. Ceram. Soc. Vol. 89 (2006), p.1122.
doi:10.1111/j.1551-2916.2005.00825.x
[93] J. Jalli, Y. Hong, S. Bae, J. Lee, G. S. Abo, J. Park, B. Choi, T. Mewes, S. Kim, S. Gee, I.T. Nam and T. Tanaka: J. Appl. Phys. Vol. 109 (2011), p. 07A509.
doi:10.1063/1.3560885
[94] J. Temuujin, M. Aoyama, M. Senna, T. Masuko, C. Ando and H. Kishi: J. Solid State. Chem. Vol. 177 (2004), p.3903.
doi:10.1016/j.jssc.2004.06.051
[96] X. He, Q. Zhang and Z. Lang: Mater. Lett. Vol. 57 (2003), p.3031.
doi:10.1016/S0016-5085(03)82945-1
[98] S. Nasir and M. Anis-ur-Rehman: Phys. Scr. Vol. 84 (2011), p.025603.
doi:10.1088/0031-8949/84/02/025603
[99] R. C. Pullar, M. D. Taylor and A. K. Bhattacharya: J. Mater. Sci. Vol. 32 (1997), p.873.
doi:10.1023/A:1018541314320
[100] K. Maruszewski, D. P. Strommen and J. R. Kincaid: J. Am. Chem. Soc. Vol. 115 (1993), p.8345.
doi:10.1021/ja00071a049
[101] R. Jotania, C. Chauhan, S. Menon and K. Jotania: Adv. Mater. Res. Vol. 67 (2009) p.137.
doi:10.4028/www.scientific.net/AMR.67.137
[106] S. Chakrabarti, S. K. Mandal and S. Chaudhuri: Nanotechnology Vol. 16 (2005) p.506.
doi:10.1088/0957-4484/16/4/029
[107] H. F. Yu and K. C. Huang: J. Magn. Magn. Mater. Vol. 260 (2003), p.455.
doi:10.1007/s00299-003-0658-x
[110] F. Wang, T. Zou, L.Q. Wan and Y. Sun: Appl. Phys. Lett. Vol. 100 (2012), p.122901.
doi:10.1063/1.3697636